SAND2016-3579C

Exceptional service in the national interest

Sandia National Laboratories

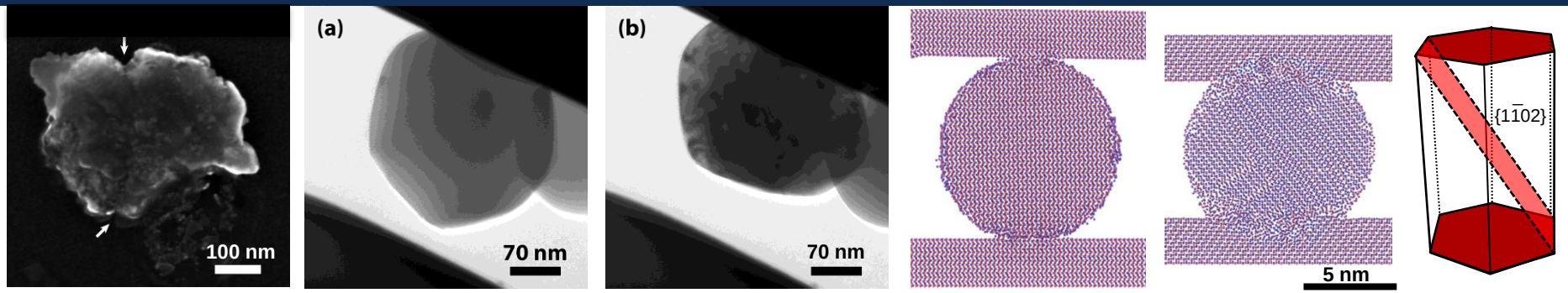

Deformation and Consolidation of Alumina Particles – Basis for Aerosol Deposition, a Room Temperature, Ceramic Deposition Process

Pylin Sarobol, Michael Chandross, William M. Mook, Paul G. Kotula, Daniel C. Bufford, Khalid Hattar, Brad L. Boyce, Jay D. Carroll, Thomas D. Holmes, Andrew S. Miller, and Aaron C. Hall

IMAPS/ACerS 12th CICMT, April 19, 2016. Denver, CO.

U.S. DEPARTMENT OF ENERGY | NNSA National Nuclear Security Administration

Building Block for Aerosol Deposited Coatings

Ceramics are conventionally processed at > 700°C. A room temperature (RT) process eliminates high processing temperature, enabling materials integration.

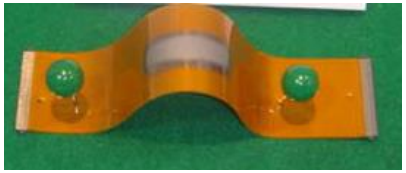

AD Flexible electronics from J. Akedo. *JTST.*, 2007:17:181

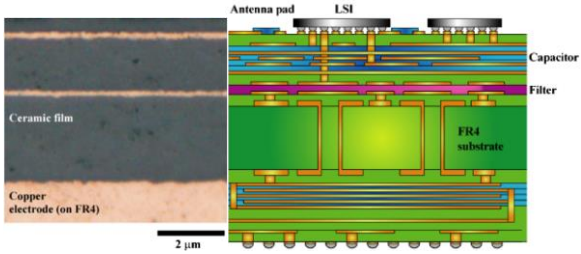

AD multi-layer capacitor from Y. Imanaka and J. Akedo. *Int. J. Appl. Ceram. Technol.* 2010:7:E23

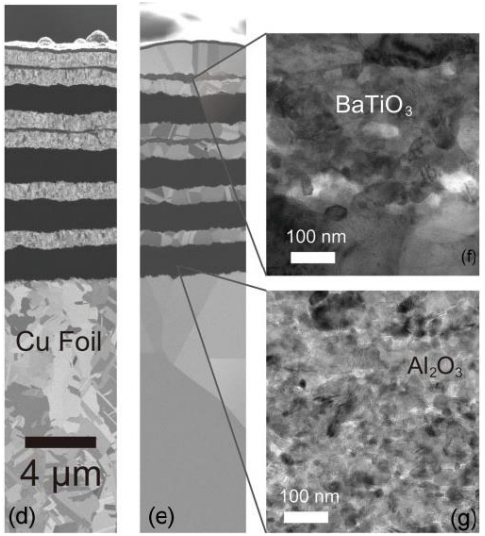

$BaTiO_3/Al_2O_3$/Cu multi-layered structure produced by AD and electroplating from Y. Imanaka *et al. Adv Engr Mater.,* 2013:15:1129

Aerosol Deposition (AD)

- J. Akedo, Y. Imanaka, D.-S. Park, C. Lee, D.M. Chun, R. Moos, S. Johnson, etc.
- AD process at RT in vacuum
  - sub-micron particles accelerated to high velocity by pressurized gas, impacted, consolidated to form films.
- Similar AD ceramic film microstructures
  - sub-micron particles undergo *plastic deformation*
  - break up into *small crystallites* (20-75 nm) [1-3]
  - planar *defects* and *amorphous regions* [4].
- Inspired by Akedo and Ogiso's work [1].

[1] Akedo, J. and Ogiso, H., *JTST*, Vol. 17, (2008), pp. 181-198.
[2] Akedo, J., *JTST*, Vol. 17, (2008), pp. 181-198.
[3] Akedo, J. *J. Am. Ceram. Soc.*, Vol. 89, (2006), pp. 1834-1839.
[4] Park, H. *et al*. Scripta Materialia, 2015.

Building Block for Aerosol Deposited Coatings

Sandia National Laboratories

Particle deformation/bonding not well understood.

Need to know how feedstock particles deform & bond.

- Common deformation mechanisms exist → Alumina
- Examine sub-micron ceramic particles RT deformation as a building block for AD coatings.
  - Quasi-static loading
    - → SEM/TEM micro-compression, MD simulations
  - High strain-rate loading
    - → impact during deposition
- Major factors affecting deposition
  - Particle materials, size, treatment
  - Substrate materials, surface roughness, etc.
  - Standoff distance, bow shock formation
  - Carrier gas type/pressure
  - Deposition chamber pressure

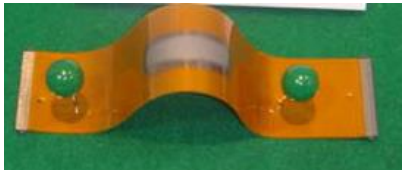

AD Flexible electronics from J. Akedo. *JTST.*, 2007:17:181

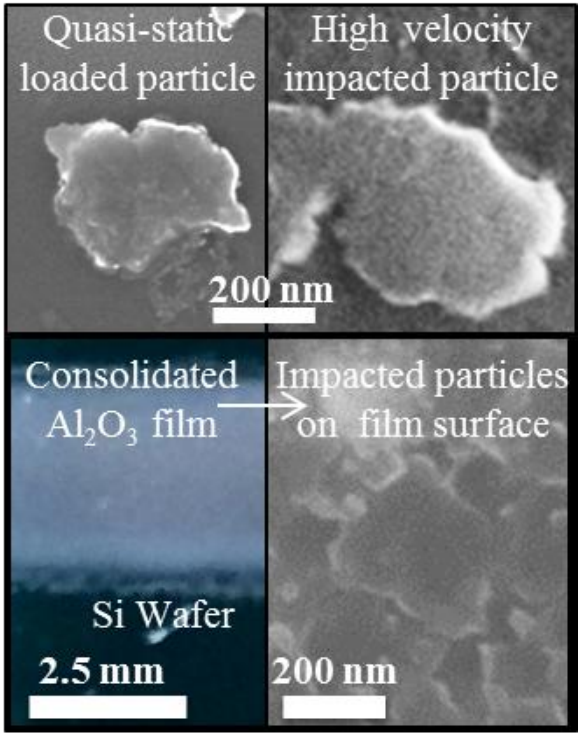

Sandia National Laboratories

How feedstock particles deform

DEFORMATION BEHAVIOR IN QUASI-STATIC LOADING

Ceramic Particle RT Deformation - Alumina

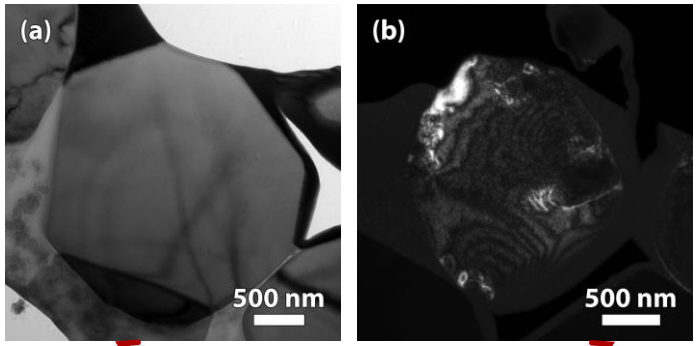

3.0μm Highly Defective

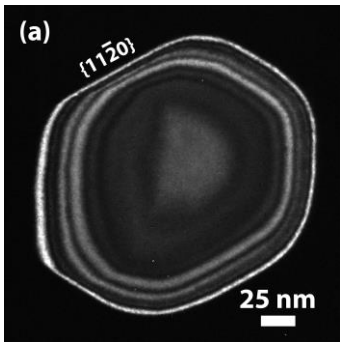

0.3μm Nearly Defect Free

Spherical Particles

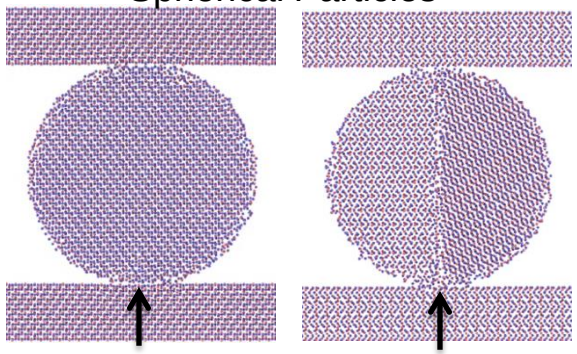

10 nm Defect Free

10 nm with a GB

- Deformation behavior influenced by *number of internal defects*, temperature, crystal orientation/size. Numbers of pre-existing (immobile) defect scale with size.
- In situ SEM/TEM micro-compression and Molecular Dynamics Simulations

Proposed

	Micron	Sub-micron	Single Crystal Nano	Bicrystal Nano
# Pre-existing Defects	High	Moderate	None	Grain Boundary
Energy Density Input	Low	Moderate	High	Low
Governing Mechanism(s)	Fracture	Plasticity + Fracture	Plasticity	Fracture
Response to Compression	Crack initiation & Propagation	Dislocation nucleation, slip, crack initiation & propagation	Dislocation nucleation, Slip	Crack initiation & propagation
Compression Testing	SEM	SEM and TEM	MD Simulation	MD Simulation

Micro-Compression Results

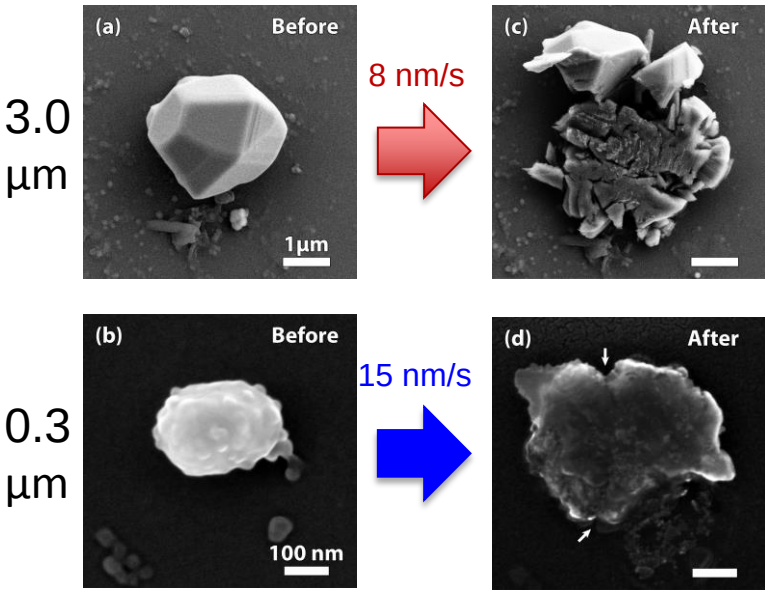

Particle Identifier	Diameter (µm)	Nominal Strain Rate (s^{-1})	Strain Energy before Fracture (MJ/m^3)	Strain at Fracture (%)
Large Particles				
SEM-LP1	2.9	0.03	47	5
SEM-LP2	2.6	0.006	106	5
SEM-LP4	2.9	0.005	70	5
SEM-LP5	2.9	0.003	203	7
Avg Large Particles	**2.8**	-	**106±69**	**5.5 ± 1**
Small Particles				
SEM-SP2	0.17	0.09	494	11
SEM-SP3	0.29	0.05	366	12
SEM-SP4	0.28	0.05	607	13
SEM-SP5	0.29	0.05	675	16
*TEM-SA2	0.38	*0.005	573	32
*TEM-SB1	0.24	*0.009	1066	27
Avg Small Particles	**0.26**	-	**630±238**	**18 ± 9**

- Micron sized particles - brittle fracture
- Sub-micron sized particles - substantial plastic deformation before fracture.
  - **6x** higher strain energy density input
    - dislocation nucleation
  - **3x** higher accumulated strain
  - In some cases, became **polycrystalline**.
- Takes more energy to nucleate dislocations and move them for deformation.

In Situ TEM Micro-Compression – 0.3µm

Sandia National Laboratories

Diameter ~ 0.24 µm, Open loop, Strain rate ~ 0.009 s^{-1}

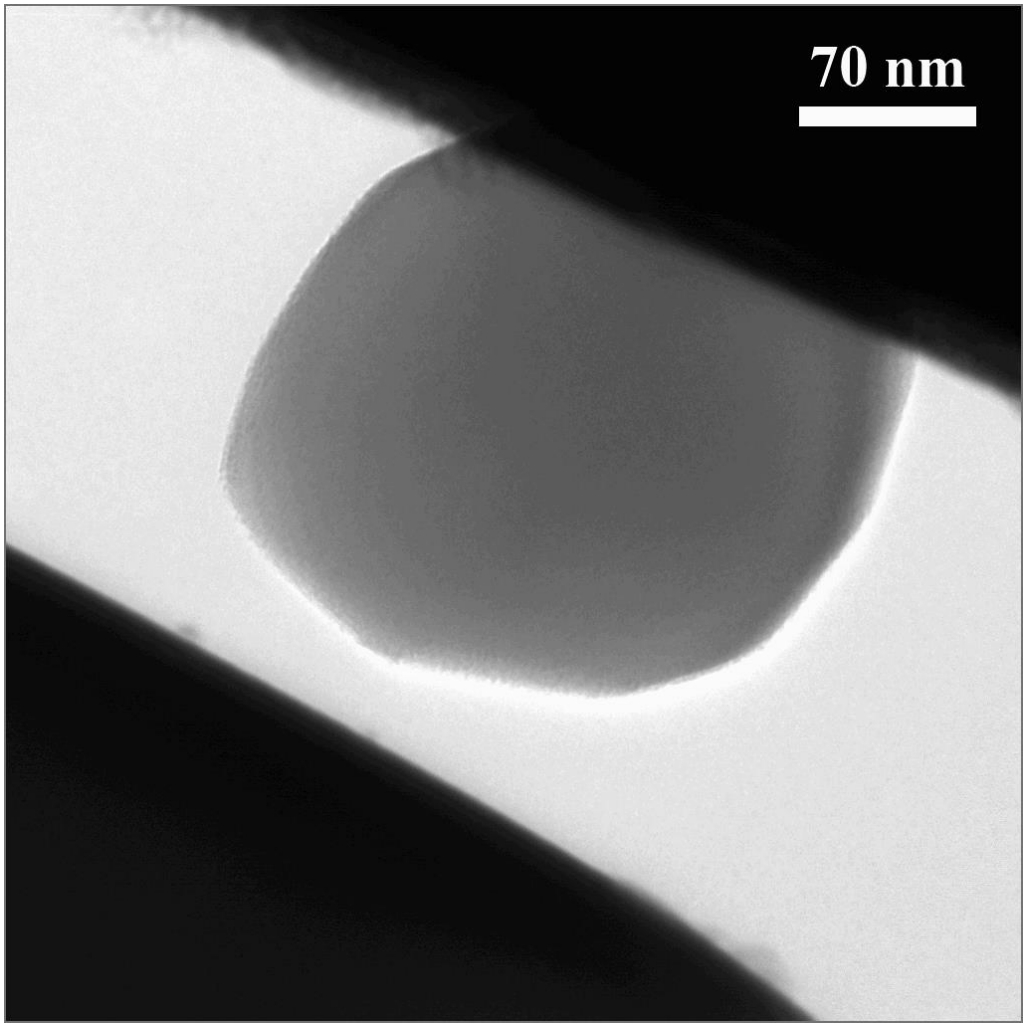

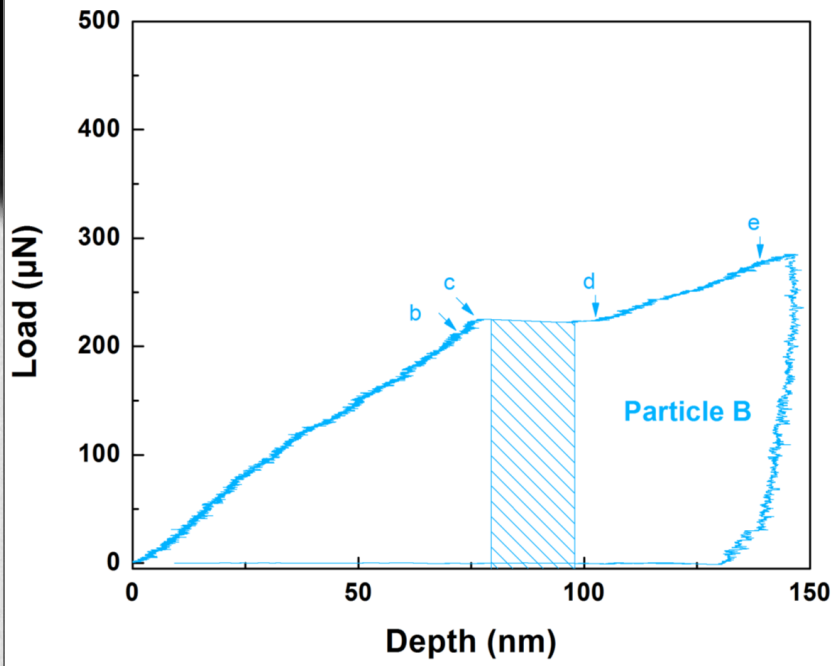

In Situ TEM Micro-Compression – 0.3µm

Sandia National Laboratories

Zone axis near $[\bar{9}\,\bar{9}\,18\,6]$

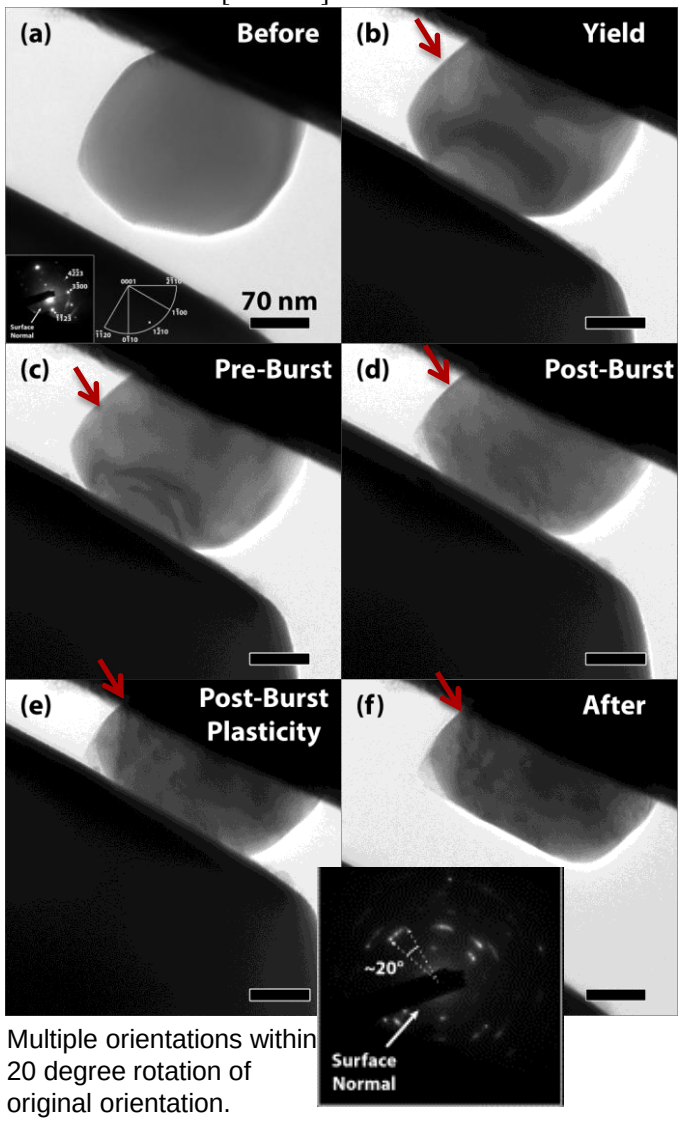

Multiple orientations within 20 degree rotation of original orientation.

- Stored Energy Density Before Fracture = 1,066 MJ/m^3

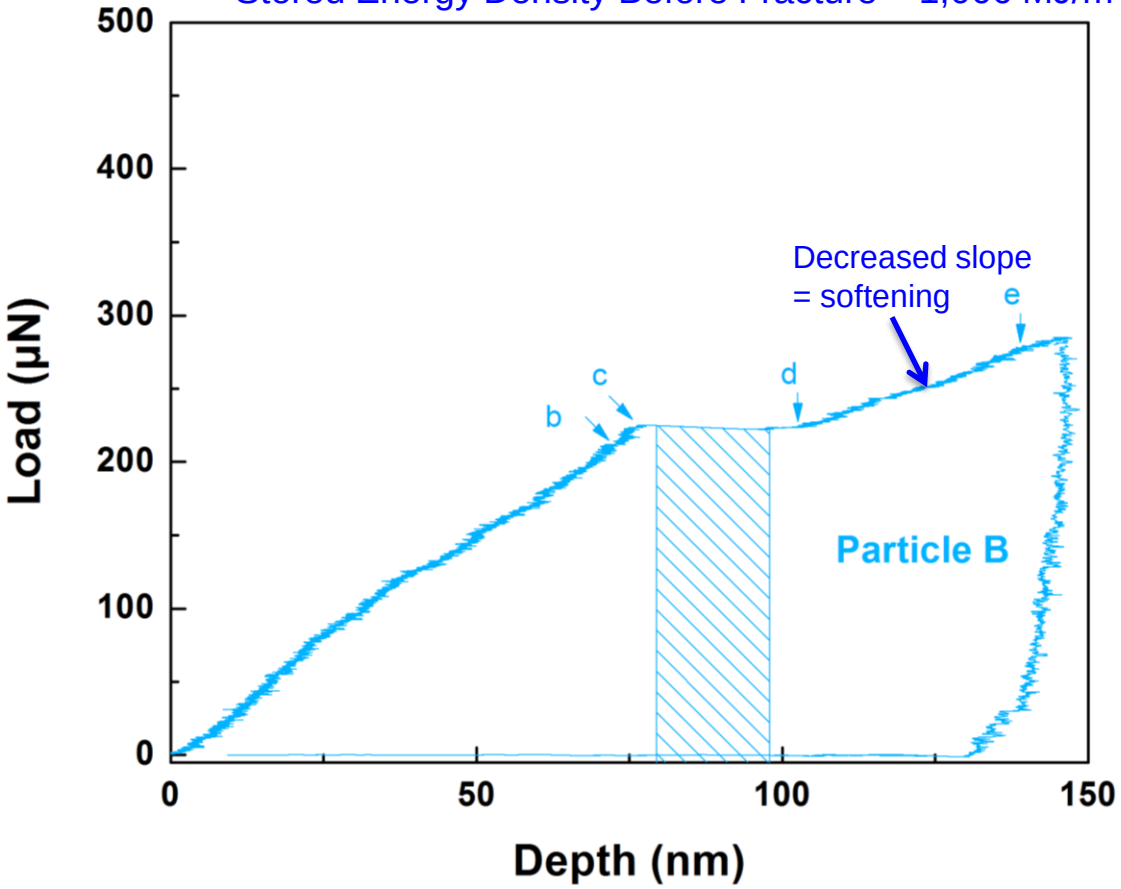

- Pre-burst plasticity: small regime with low dislocation activity.
- Post-burst plasticity: high dislocation activities, change in deformation mechanism as indicated by lower slope.
- **Mosaicity** with a 20 degree orientation spread.

Simulated Particle Compression

MD Simulations – 10 nm nanoparticles (NPs)

- Infeasible (long computing time) to simulate size >0.05µm
- TEM examination showed that 'smaller' particles (0.3µm) are nearly defect-free, and 'larger' particles (3.0µm) contain immobile defects.
- Circumvented the size limitation of our models by simulating similar sized (10 nm) nanoparticles (NPs) that were either single crystal or contained an internal grain boundary (GB) as an initial immobile defect.
- Hypothesis: Pre-existing defects influence behaviors
  - The defect-free single crystal NP will require higher energy density input to nucleate and glide dislocations.
  - The NP with a grain boundary (GB) as immobile defect will require less energy density input for crack initiation at the GB.
- A force-field for ceramics, developed by Garofalini[8].
- NPs were compressed (by ~1/3 of the initial diameter) between single crystal α-Al_2O_3 walls at a constant velocity of **20 m/s**.

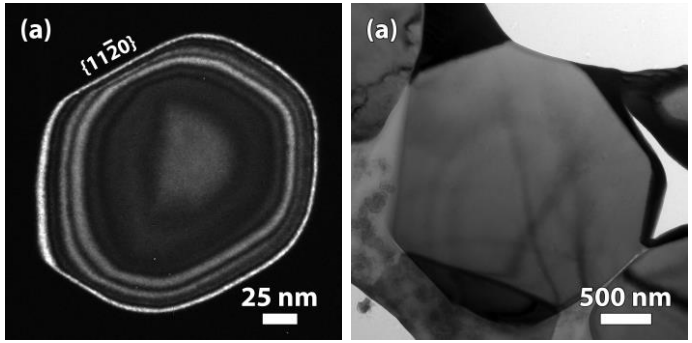

0.3µm Nearly Defect Free 3.0µm with GB

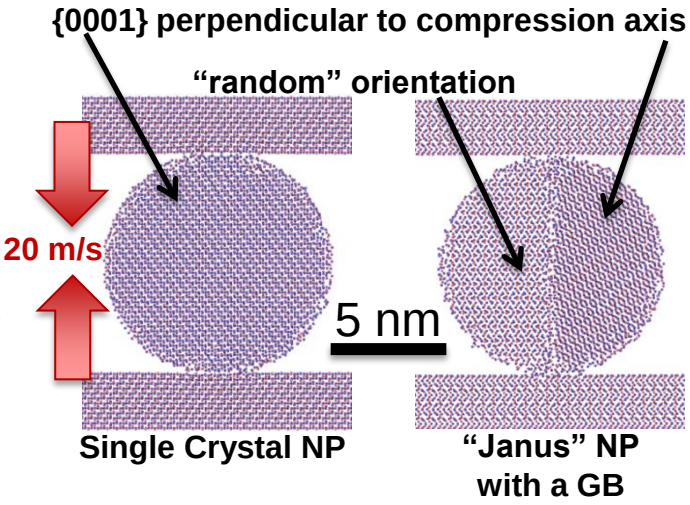

[8] Blonski, S. and Garofalini, S. H., *J. Phys. Chem.*, Vol. 100, (1996), pp. 2201-2205.

MD Simulation Results

Defect-free single crystal NP

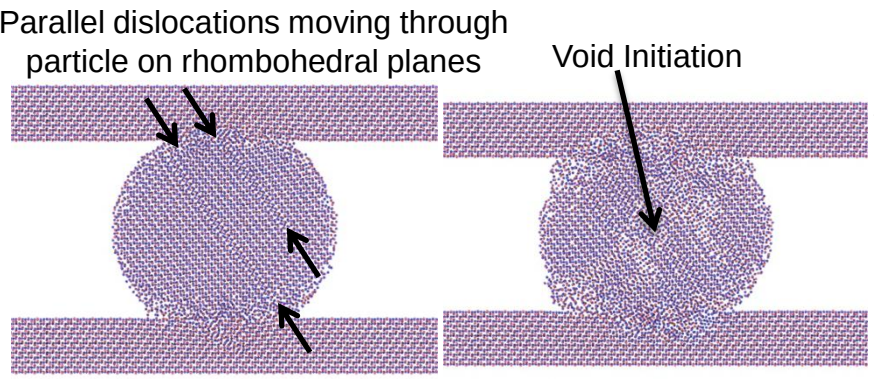

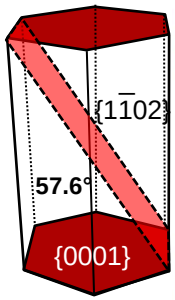

'Janus' NP containing a grain boundary

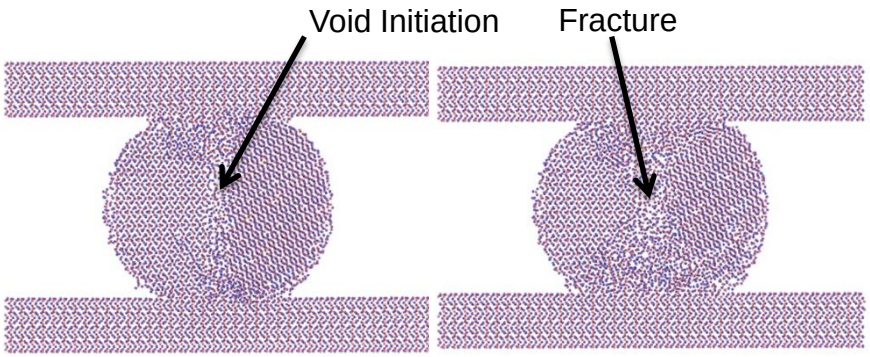

- The energy to fracture is larger for single crystal NP by a factor of **2.9x**.
  - Energy for both dislocation nucleation/movement *and* fracture
  - factor of **6x** from experiment.
- The strain to first fracture is larger for single crystal NP by a factor of **1.5x**
  - factor of **3x** from experiment.
- Experiments and simulations agree.
- Takes more energy to nucleate dislocations and move them for deformation.

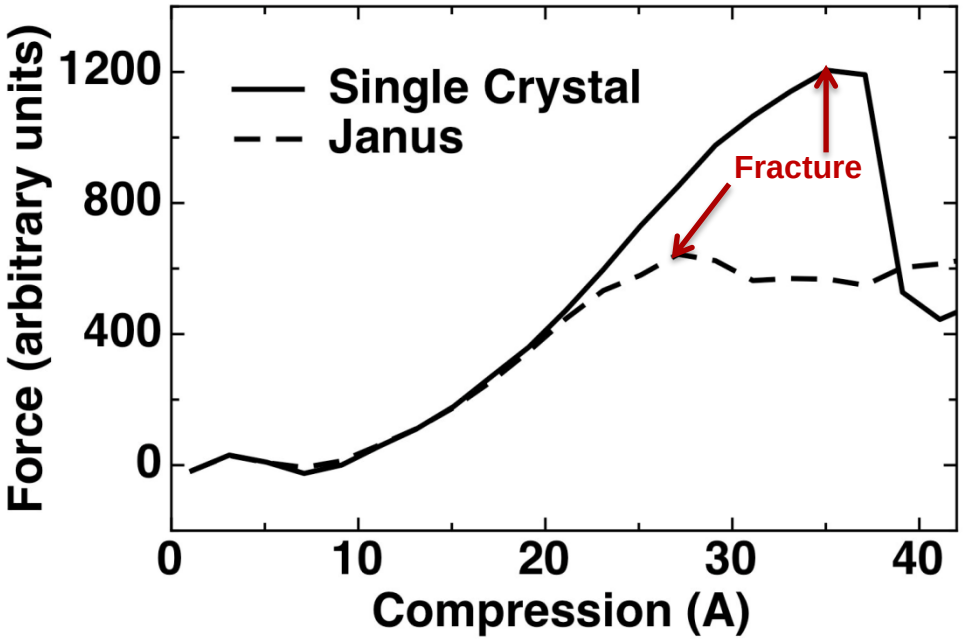

MD Simulation Results

Sandia National Laboratories

10 nm diameter, defect-free, single crystal α-alumina, compression axis ⊥ (0001)

20 m/s → dislocation nucleation, coordinated shear, fracture

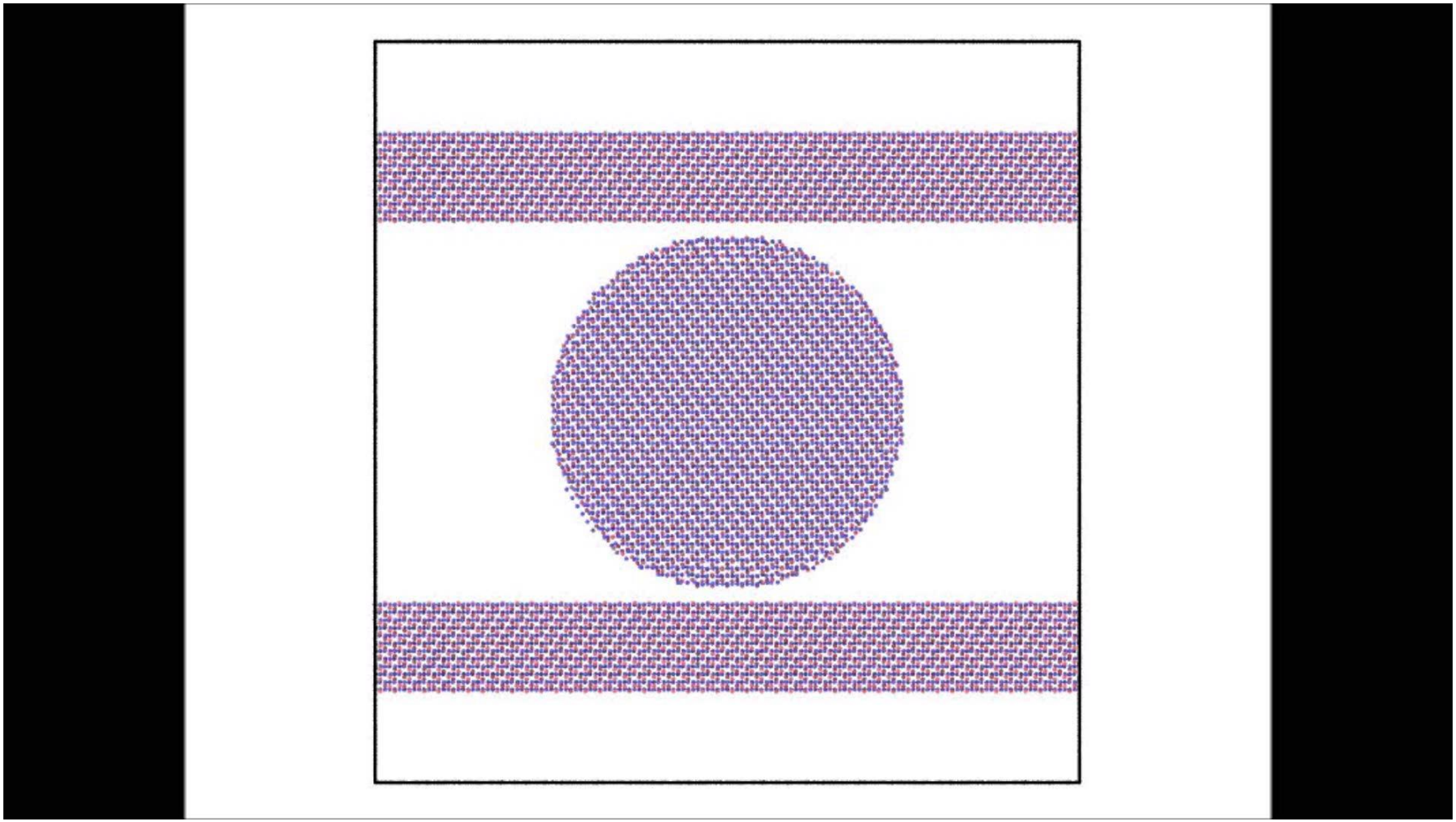

MD Simulation Results

10 nm diameter, contain a GB, 'Janus' α-alumina,
20 m/s, left side randomly oriented and right side compression axis ⊥ (0001) → Fracture

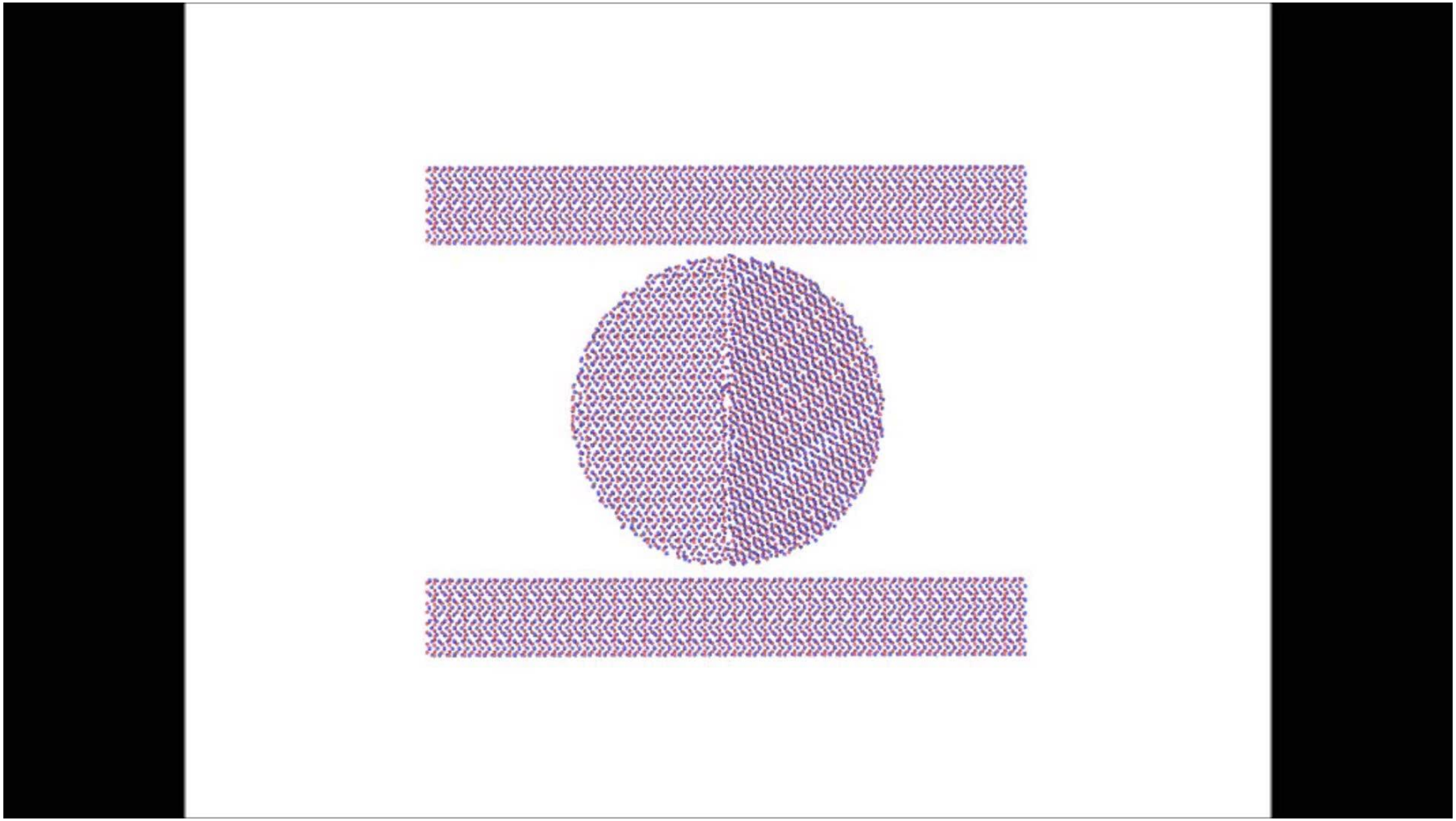

RT Deformation Mechanisms

- Deformation behavior influenced by numbers of internal defects, orientation, size.

Verified

	Micron	Sub-micron	Single Crystal Nano	Bicrystal Nano
# Pre-existing Defects	High	Moderate	None	Grain Boundary
Energy Density Input	Low	Moderate	High	Low
Governing Mechanism(s)	Fracture	Plasticity + Fracture	Plasticity	Fracture
Response to Compression	Crack initiation & Propagation	Dislocation nucleation, slip, crack initiation & propagation	Dislocation nucleation, Slip	Crack initiation & propagation
Compression Testing	SEM	SEM and TEM	MD Simulation	MD Simulation

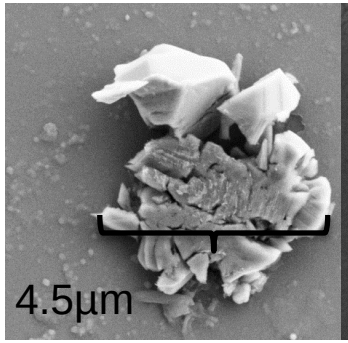

3.0µm - Fracture and Fragmentation

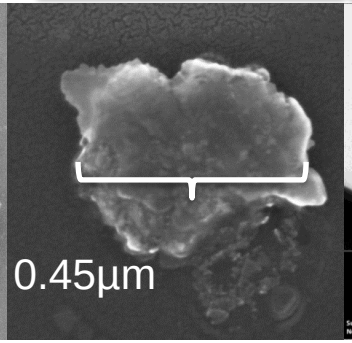

0.3µm – plastic deformation, shape change, cracking

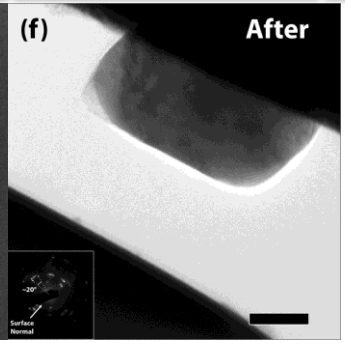

0.3µm – Dislocation Plasticity & Fracture - Polycrystalline

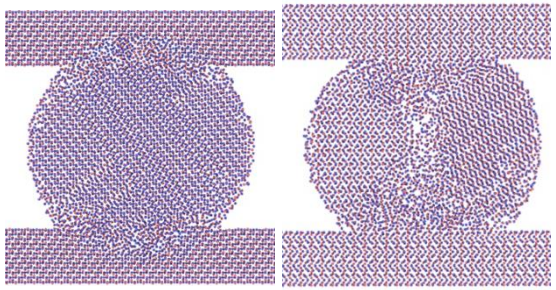

10 nm – Dislocation Plasticity **10 nm - Fracture**

- Interesting finding = higher absorbed energy needed to nucleate and move dislocations.

RT Deformation Mechanisms

Akedo and Lebedev, Jpn. J. Appl. Phys. 2002:**41**;6980

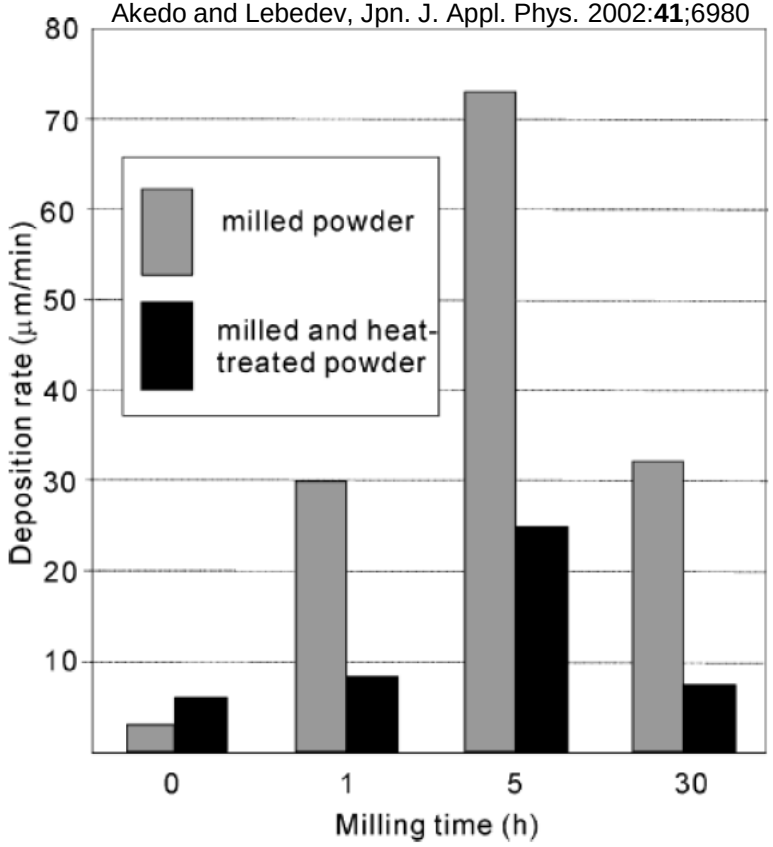

Fig. 4. Deposition rate for PZT film formation at room temperature using powder milled for different duration times with (black bar)/without (gray bar) heat-treatment procedure at 800°C for 4 h in air. The deposition area is 5 × 5 mm^2.

Sub-micron	Single Crystal Nano
Moderate	None
Moderate	High
Plasticity + Fracture	Plasticity
Dislocation nucleation, slip, crack initiation & propagation	Dislocation nucleation, Slip
SEM and TEM	MD Simulation

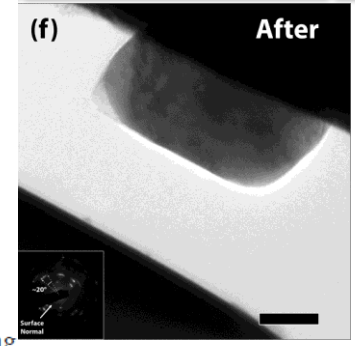

0.3μm – Dislocation Plasticity & Fracture - Polycrystalline

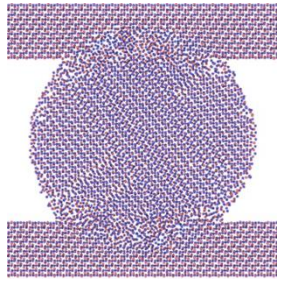

10 nm – Dislocation Plasticity

- Ball milled particles contain mobile dislocations deform more easily at lower particle velocity during impact.
- Annealing ball milled particles was shown to cause polygonization—dislocation alignment to form subgrains—which was shown to increase deposition efficiency in the AD coating process (Park et al. *JTST*, 2013:**22**;882).

Sandia National Laboratories

How feedstock particles bond

DEFORMATION BEHAVIOR IN HIGH STRAIN-RATE LOADING

Aerosol Deposition

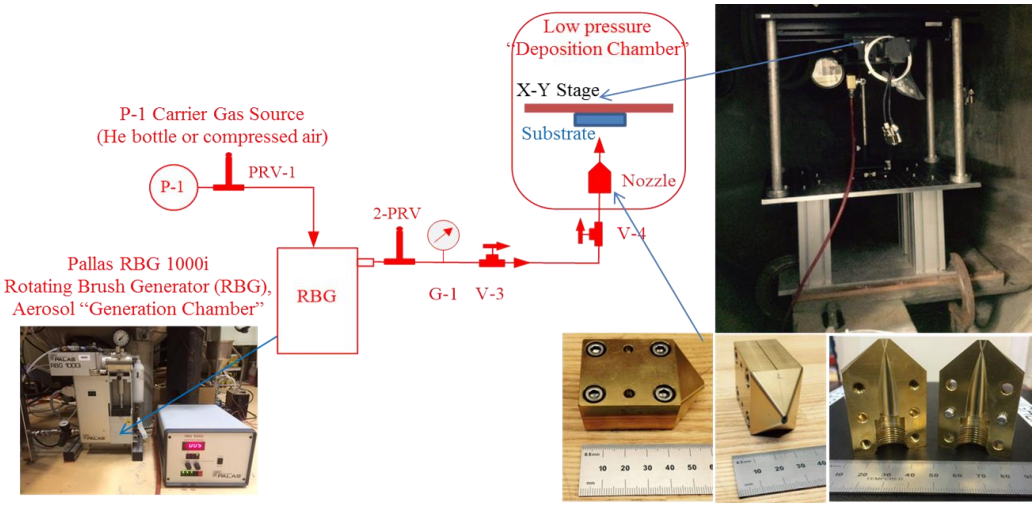

Aerosol delivery and deposition system at Sandia National Laboratories

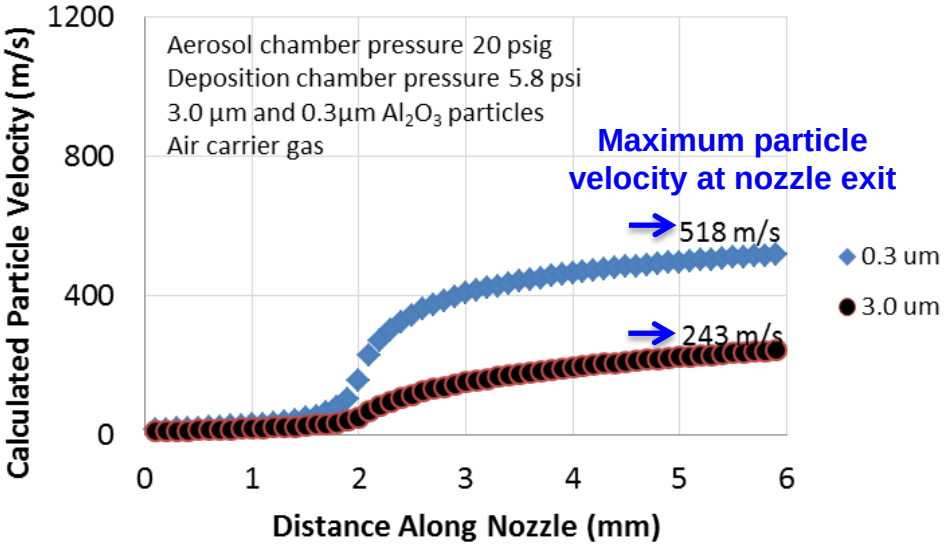

Predicted particle velocity using a particle laden flow model originally developed for calculating a 1-D particle velocity in cold and plasma spray processes by Dykhuizen et al.

- Nozzle adapted from D.M. Chun and S.H. Ahn. *Acta Mater*, 2011:59;2693.
- SNL particle laden flow model predicts
  - choked flow is achieved when aerosol chamber > 5psi.
  - particle velocity in the nozzle is unaffected by the deposition chamber pressure (similar velocities predicted for <5.8 psi).
- Deposition Conditions
  - Air or He carrier gas
  - Sapphire, YSZ, Si substrates
  - Standoff distance 5-10mm
  - Stage Traverse Speed 5-20 mm/s
  - Aerosol chamber 5-25 psi
  - Deposition chamber 0.005-5.8 psi

Single Particles Deposition - Alumina

- Sapphire substrate
- Dents – impact from the 3.0µm particles
- Splats – impacted and adhered 0.3µm particles

Carrier Gas = Air
Aerosol Chamber = 20 psig.
Deposition Chamber = 5.8 psi.
Standoff Distance = 5 mm.
Run time = 15 minutes

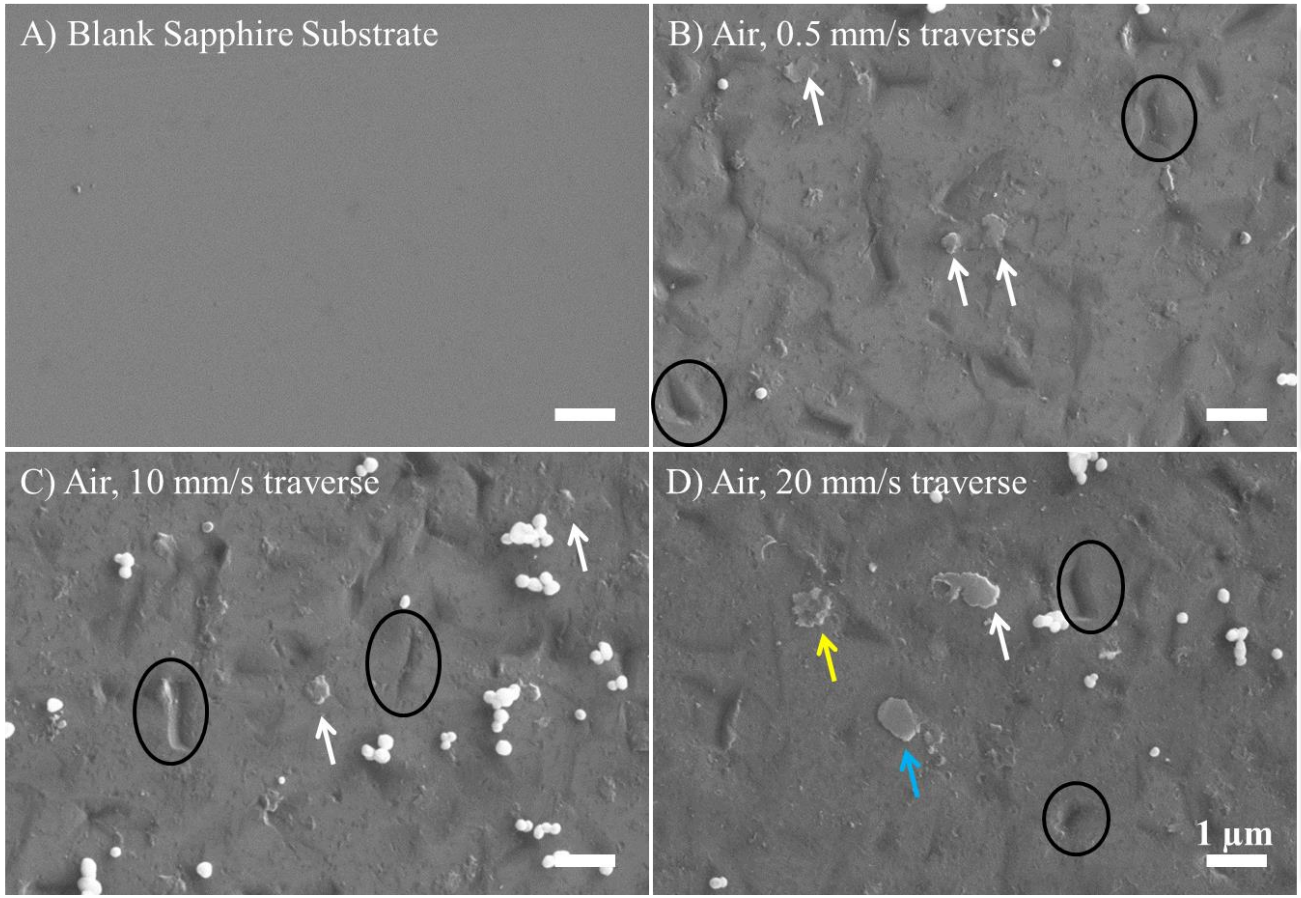

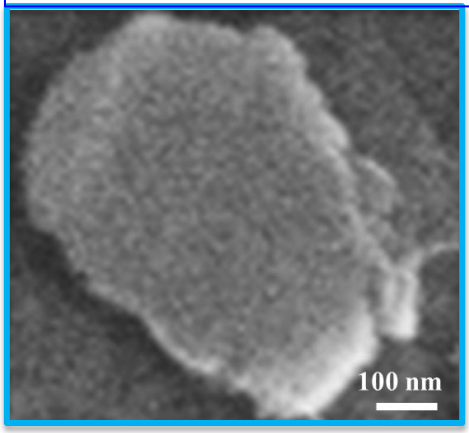

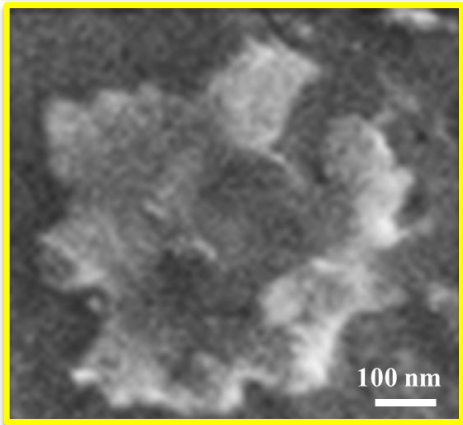

Single Particles Deposition - Alumina

- undisturbed substrate area free of defects
- Impacted substrate area full of dislocations
- observed regions with bonding towards the middle of the particle and regions containing gaps towards the outer edge of the particle.

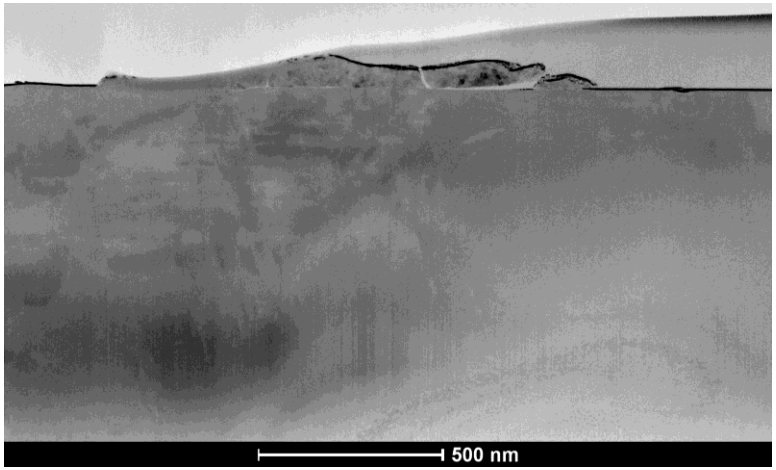

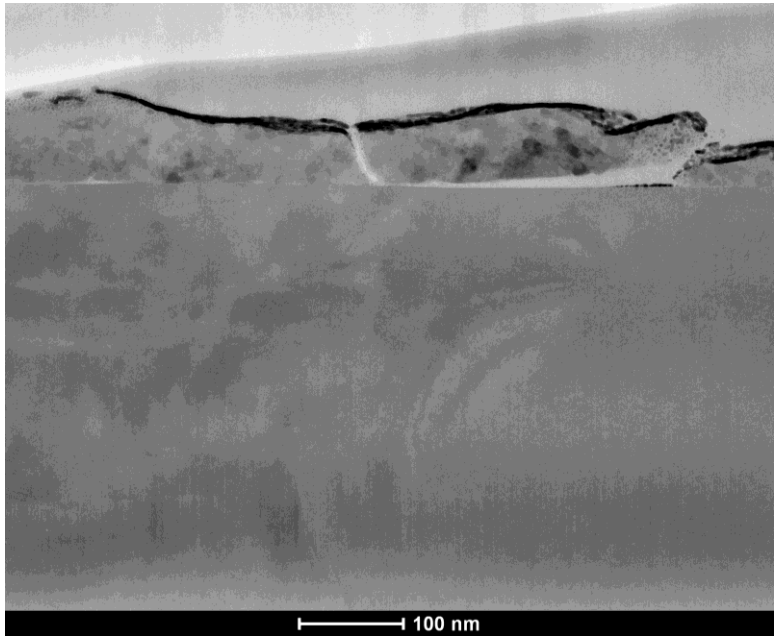

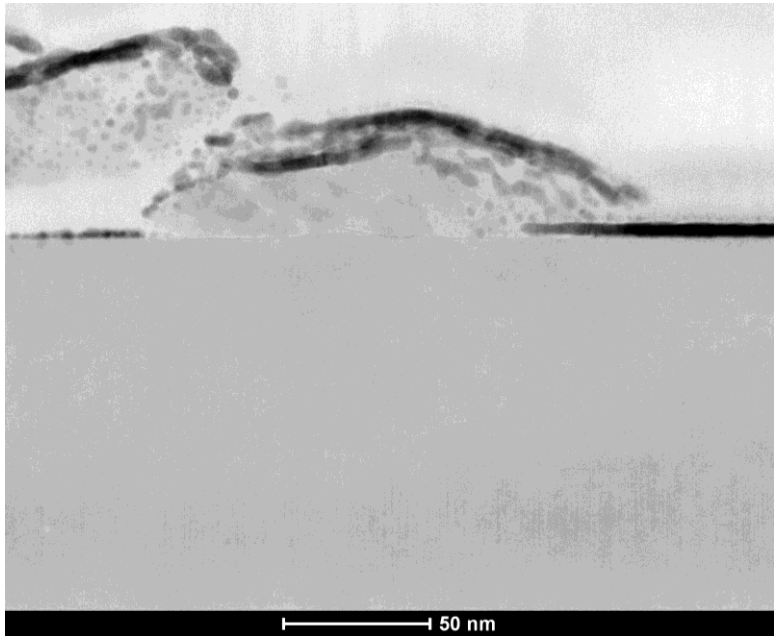

Single Particles Deposition - Alumina

- undisturbed substrate area free of defects
- Impacted substrate area full of dislocations
- observed regions with bonding towards the middle of the particle and regions containing gaps towards the outer edge of the particle.
- Diffraction pattern revealed that the splat is polycrystalline with mosaicity

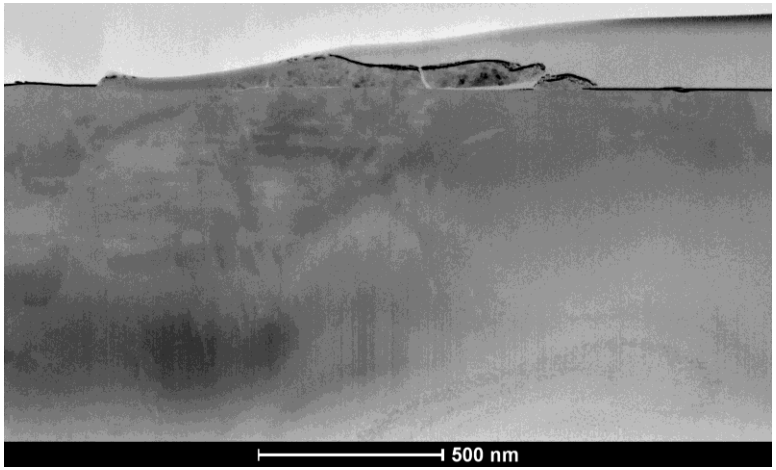

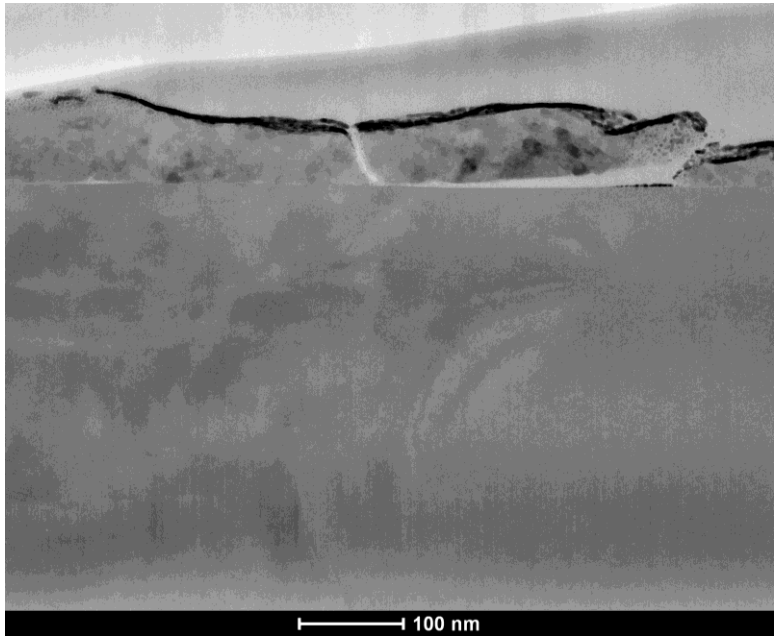

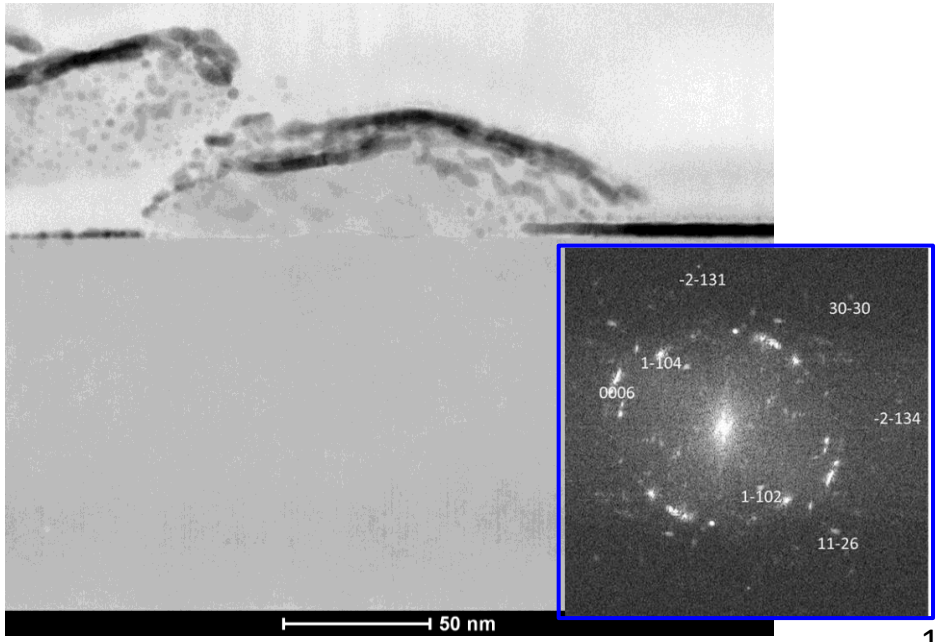

Single Particles Deposition - Alumina

- Bonded area showed a very small disordered layer at the particle/substrate interface.
- Splatted particles deformed and fractured into many subgrains (15-30 nm), without fragmentation.
- Non-bonded area showed <5 nm gap.

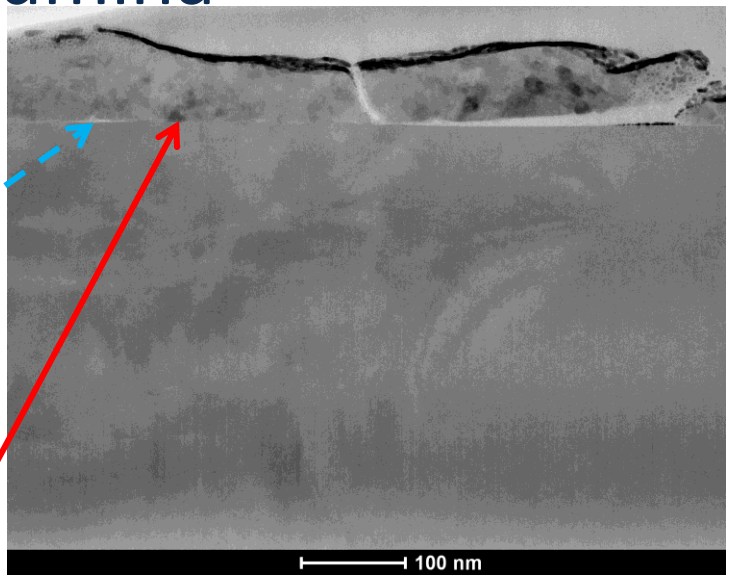

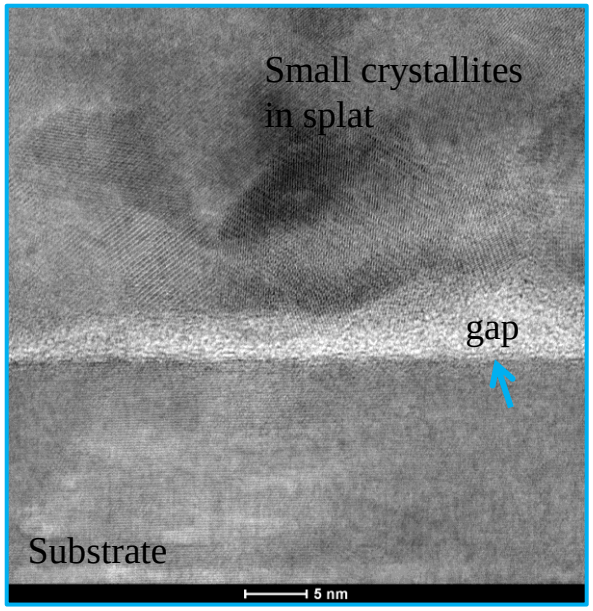

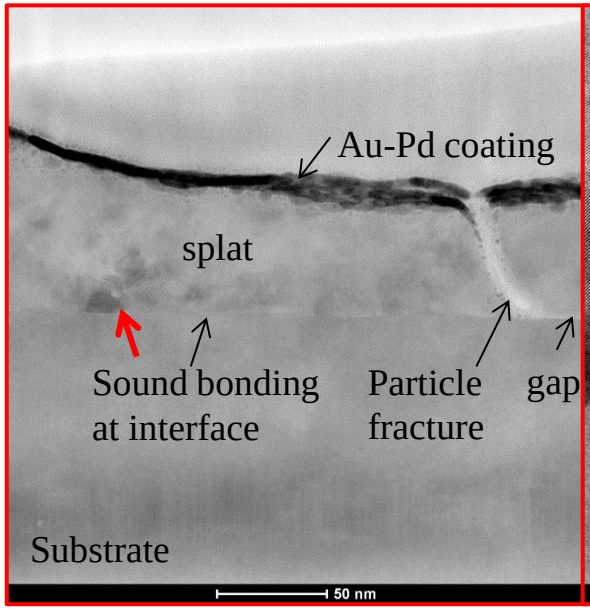

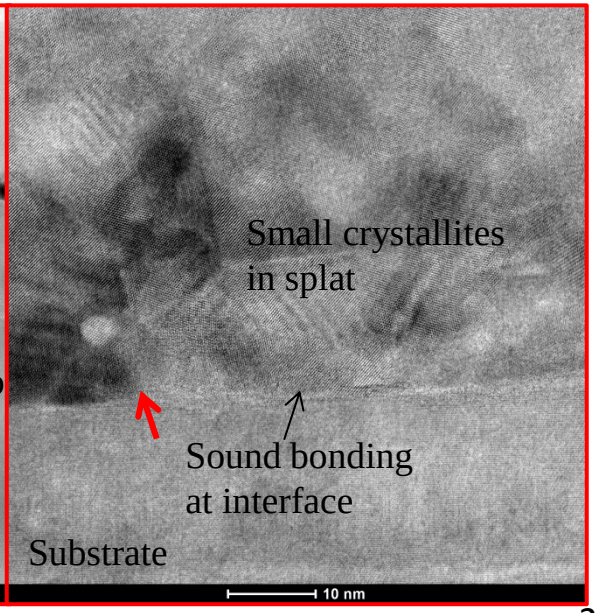

Coating Deposition - Alumina

- Sapphire Substrate
- Effects of carrier gas type/aerosol chamber pressure
  - 20 psig air → no coating
  - 5 psig He → coherent coating with some pin holes
  - 20 psig He → coherent coating

Carrier Gas = Air or He
Aerosol Chamber = 5 or 20 psig.
Deposition Chamber = 5.8 psi.
Standoff Distance = 5 mm.
Run time = 15 minutes

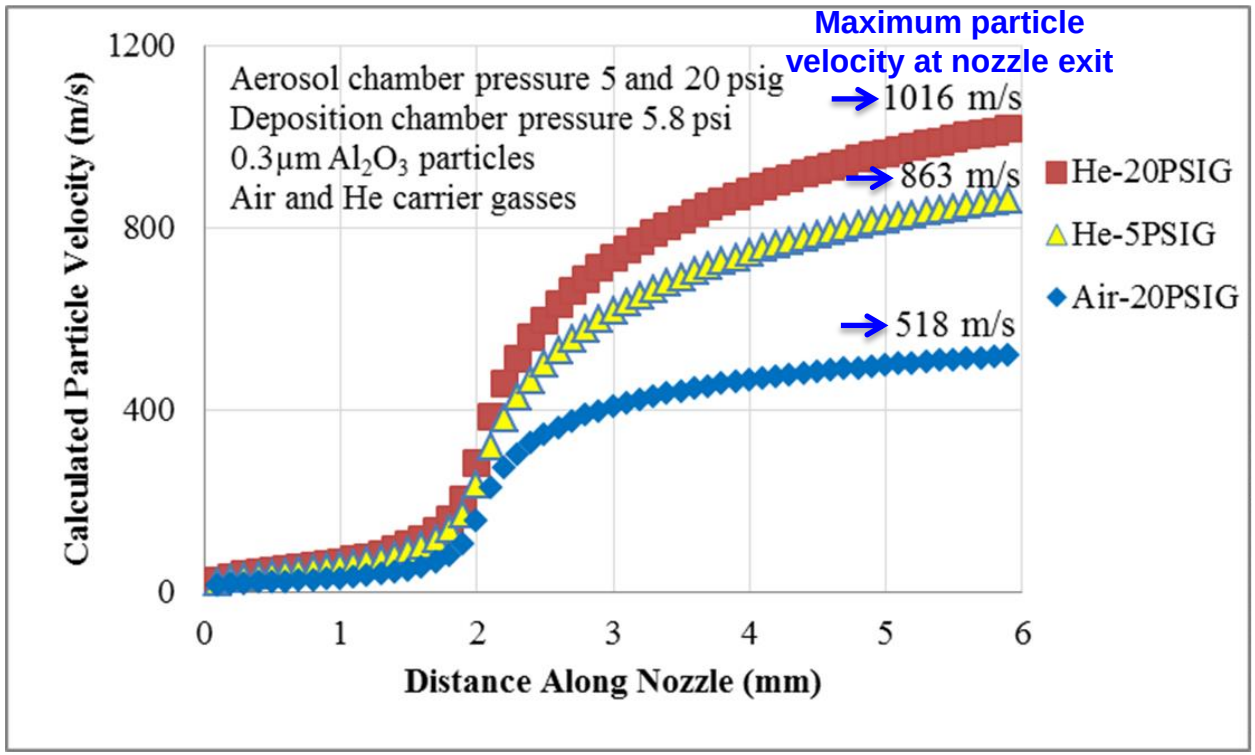

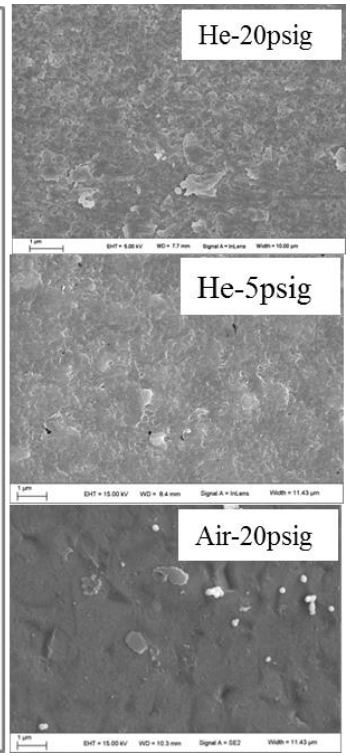

Coating Deposition - Alumina

- Interface almost indistinguishable
- Nanocrystalline coating ~100-150nm thick.
- The kinetic energy facilitated deformation and chemi-mechanical particle-substrate bonding.
- "Tamping Effect" [1-4].

Carrier Gas = He
Aerosol Chamber = 25 psig.
Deposition Chamber = 0.05 psi.
Standoff Distance = 5 mm.
Run time = 15 minutes

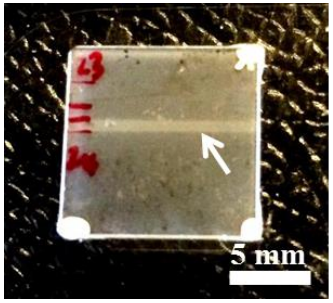

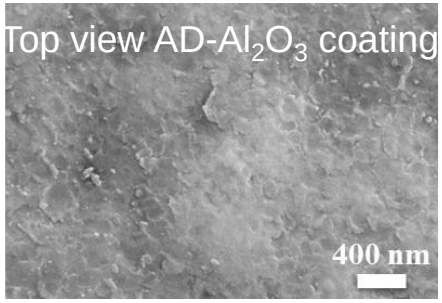

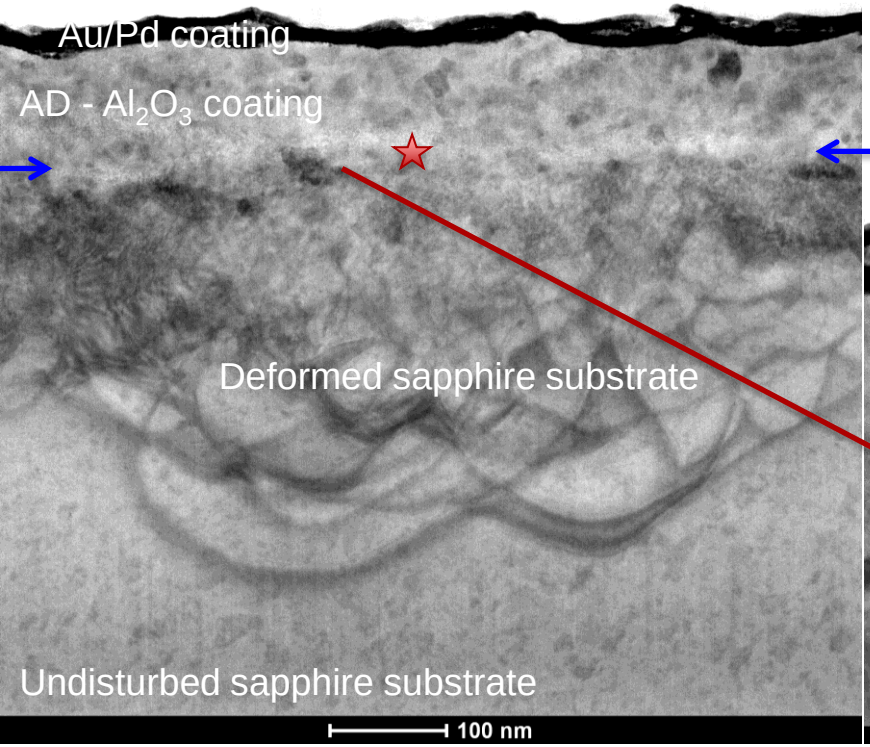

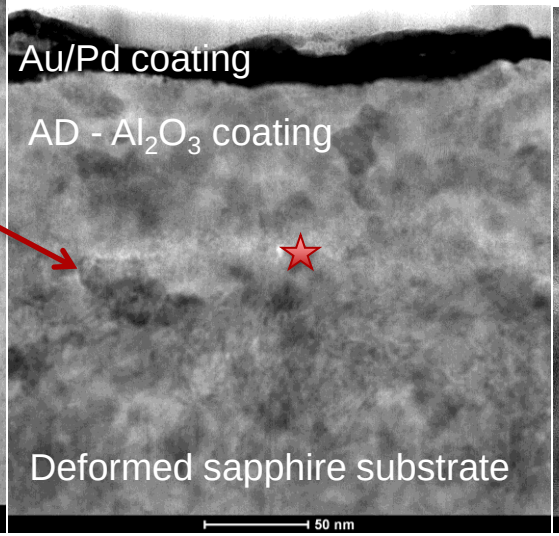

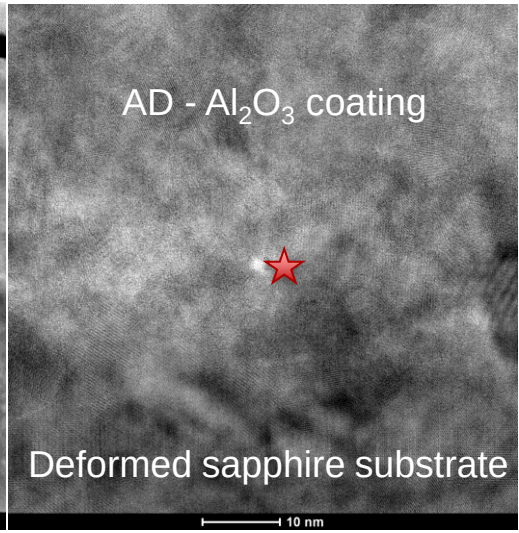

[1] H. Park, et al. *JTST*, 2013:**22**;882. [2] Y.-Y. Wang et al. *JTST*, 2010:**19**;1231
[3] F. Cao, et al. *JTST*, 2013:**22**; 1109 [4] S.-Q. Fan, et al. *JTST*, 2006:**15**;513

Coating Deposition - Alumina

- "Tamping Effect" [1-4].
- See more tamping effect on the coating surface using 100% He gas vs. 50%He-50% Air.

Carrier Gas = He or He + Air
Aerosol Chamber = 25 psig.
Deposition Chamber = 0.05 psi.
Standoff Distance = 5 mm.
Run time = 15 minutes

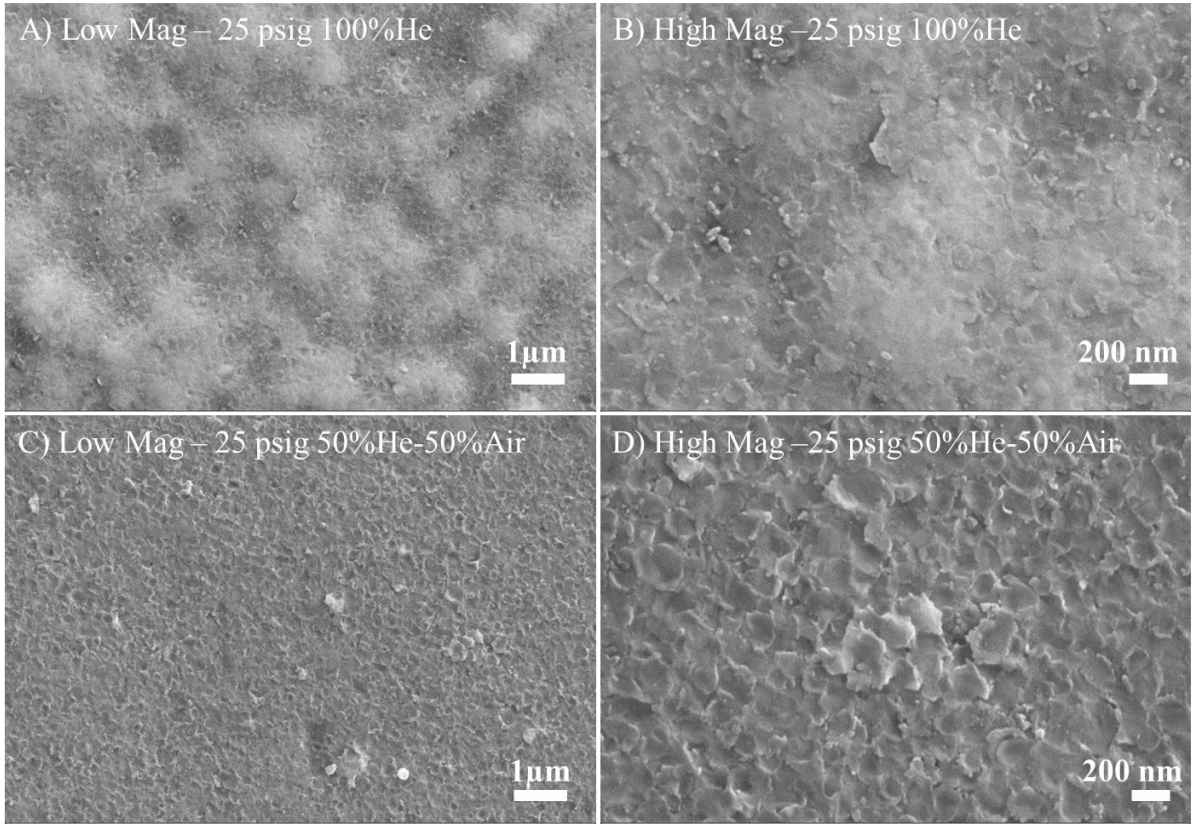

[1] H. Park, et al. *JTST*, 2013:**22**;882. [2] Y.-Y. Wang et al. *JTST*, 2010:**19**;1231
[3] F. Cao, et al. *JTST*, 2013:**22**; 1109 [4] S.-Q. Fan, et al. *JTST*, 2006:**15**;513

Sandia National Laboratories

From Particle Quasi-Static and High Strain Rate Loadings, as well as Deposition Experiments Results

PROPOSED DEFORMATION AND BONDING MECHANISMS FOR AD

Summary of Results

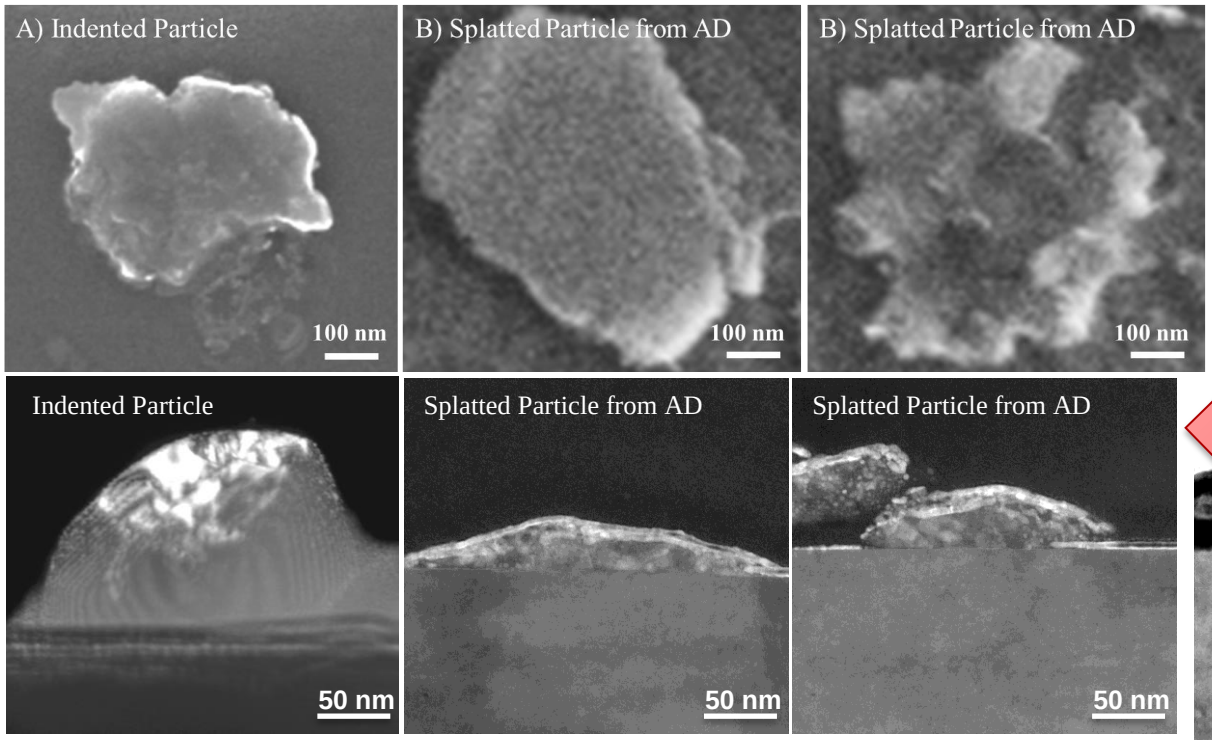

- Observed similar microstructural characteristics in the indented particles and the splatted particles.
- "Tamping" from subsequent impacting particles build up dense coating.

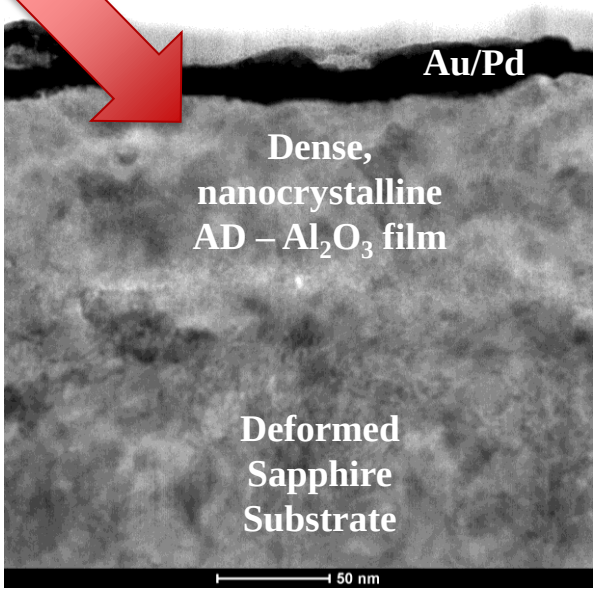

In both quasi-static and high strain-rate loadings, 0.3μm feedstock particles underwent plastic deformation

- dislocation nucleation and slip
- shape change
- fracture into nanocrystals (15-30nm)
- polycrystalline with mosaicity

RT Deformation & Bonding Mechanisms

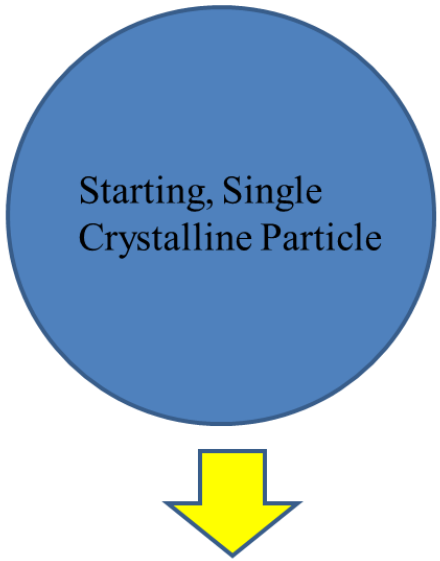

RT Deformation & Bonding Mechanisms

Sandia National Laboratories

Kinetic Energy converted to absorbed strain energy, providing

- Dislocation plasticity to deform particle
- Fracture - nanocrystalline formation in particle
- Chemi-mechanical bond between particle-substrate

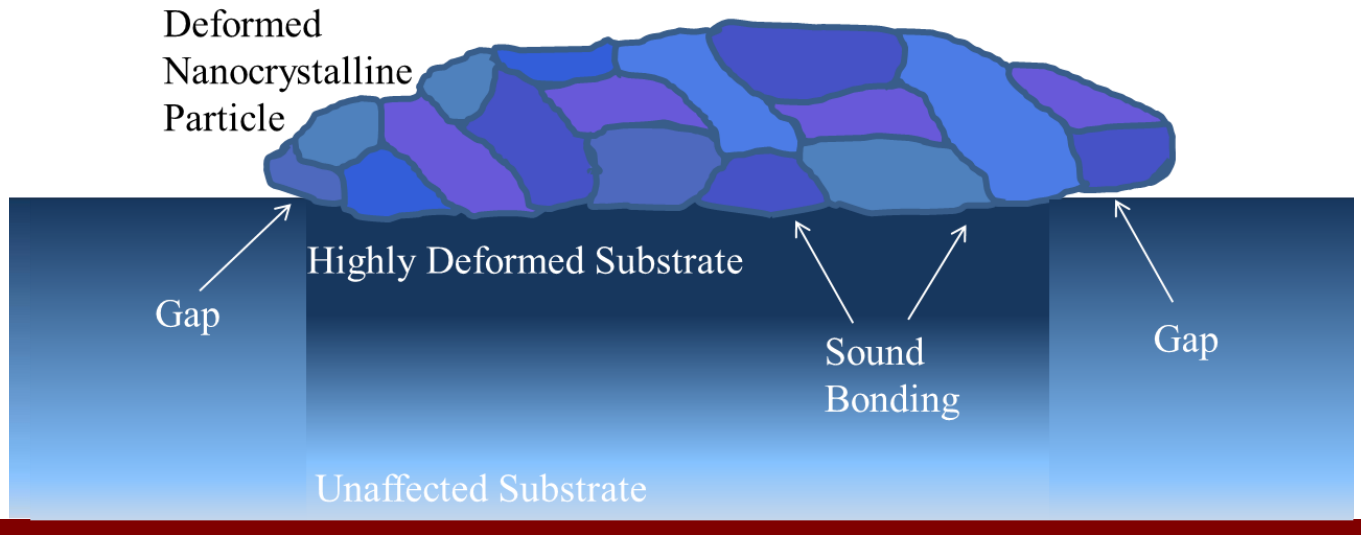

RT Deformation & Bonding Mechanisms

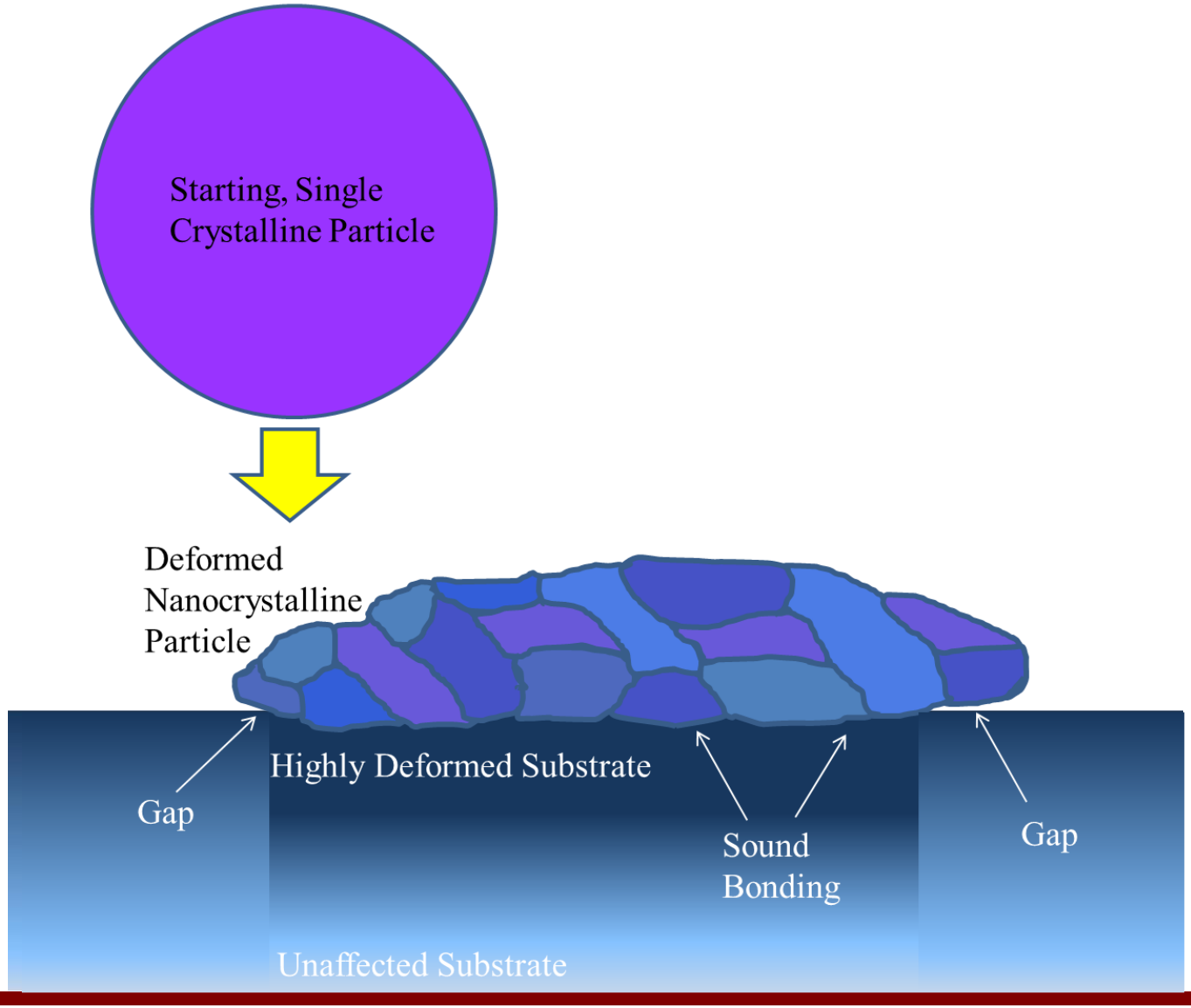

RT Deformation & Bonding Mechanisms

Sandia National Laboratories

Subsequent impacting particle imparts sufficient energy to

- Further deform splatted particle
- Provide further bond formation between splatted particle-substrate from “tamping effect”
- Compaction and densification of deposited coating from “tamping effect”

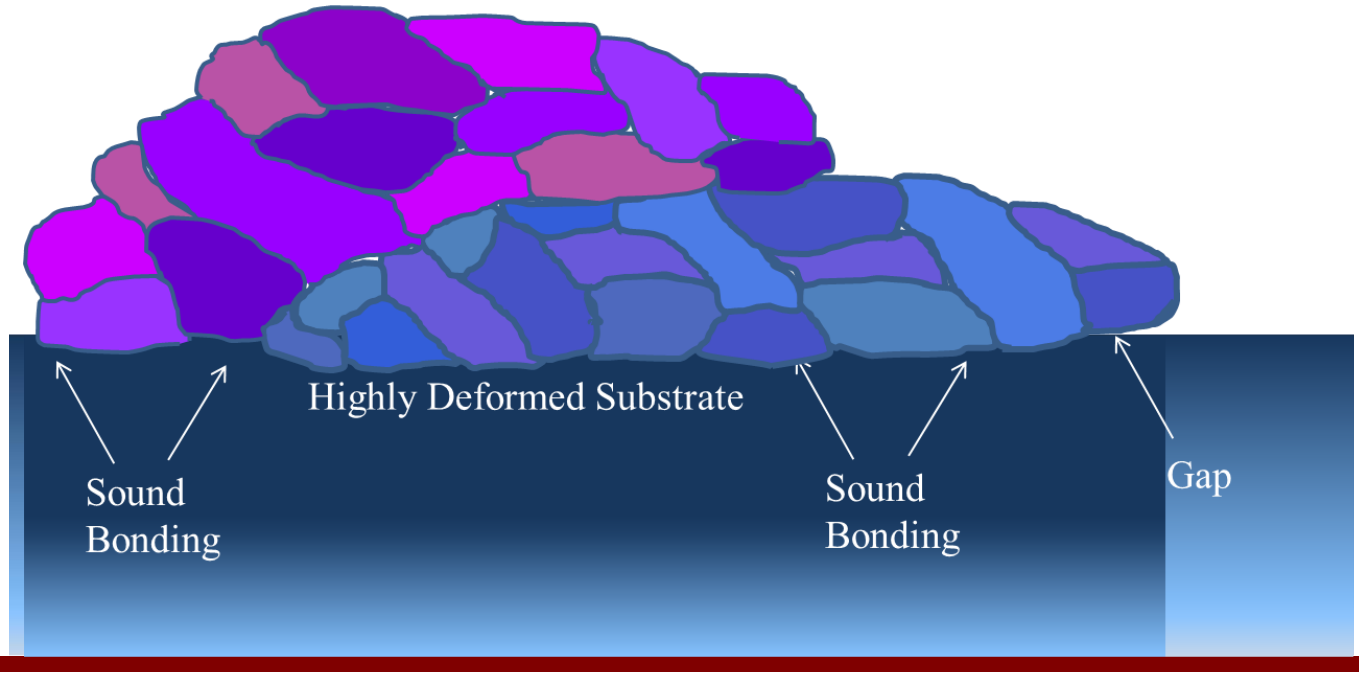

Conclusions

- AD Feedstock - submicron particles
  - capable of plastic deformation
  - Dislocation nucleation, slip, fracture without fragmentation
    - Quasi-static compressive loading at low strain rates.
    - Impact induced compressive loading at high strain rates
- Ball milled feedstock - higher deposition efficiency
  - Provide pre-nucleated mobile dislocations
  - ↓ strain energy (↓particle velocity) needed during deposition
- Tamping Effect – particle/substrate and particle/particle bonding
  - close the gaps and allow anchor layer to form complete bond to the substrate.
  - Further deform, fracture, and mechanically bond the arriving particles to the already deposited particles.
  - Select appropriate carrier gas type and pressure to control tamping, film density, and residual stress

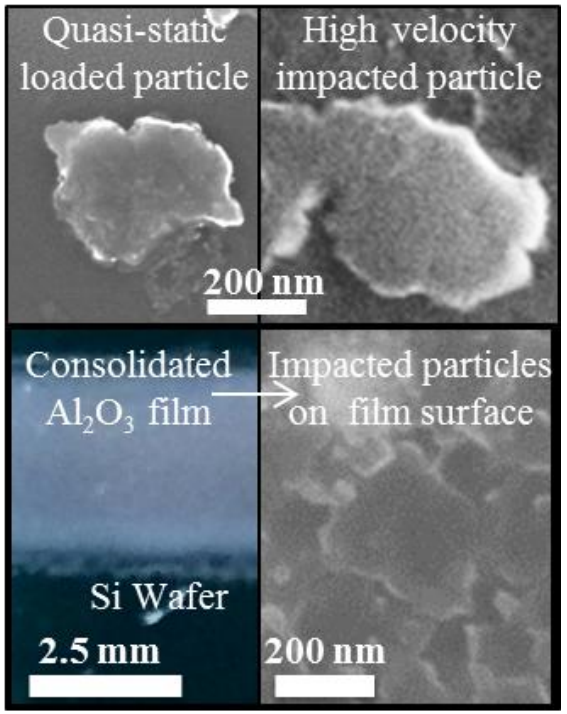

- **The knowledge gained from this work provides a strong foundation to mature the SNL aerosol deposition process for fabricating ceramic films on metallic, glass, and plastic substrates at RT**

Thank you for your attention.

Pylin Sarobol – psarobo@sandia.gov

Sandia National Laboratories

BACK UP SLIDES

Ceramic Particle RT Deformation - Alumina

- Deformation behavior influenced by *number of internal defects*, temperature, crystal orientation/size. Numbers of pre-existing (immobile) defect scale with size.
- In situ SEM/TEM micro-compression and Molecular Dynamics Simulations

Proposed

	Micron	Sub-micron
# Pre-existing Defects	High	Moderate
Energy Density Input	Low	Moderate
Governing Mechanism(s)	Fracture	Plasticity + Fracture
Response to Compression	Crack initiation & Propagation	Dislocation nucleation, slip, crack initiation & propagation
Compression Testing	SEM	SEM and TEM

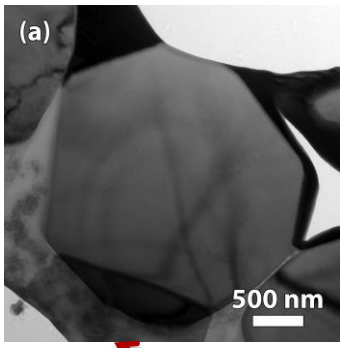

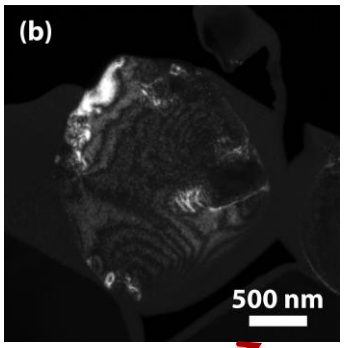

3.0μm Highly Defective

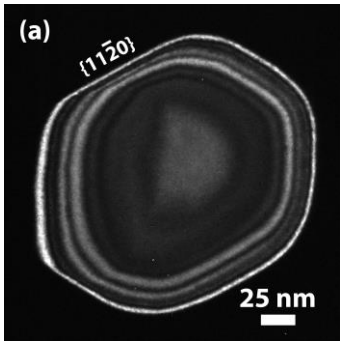

0.3μm Nearly Defect Free

- Infeasible (long computing time) to perform molecular dynamics simulations on size >0.05μm
- 'smaller' particles (0.3μm) are nearly defect-free, and 'larger' particles (3.0μm) contain immobile defects that serve as crack nucleation sites.
- Circumvented the size limitation of our models by simulating similar sized (10 nm) nanoparticles (NPs) that were either
  - single crystal
  - contained a grain boundary (GB) as an initial immobile defect.
- This approach still enables the study of NP deformation/fracture in computationally-feasible systems.

Micro-Compression Experiments

Sandia National Laboratories

In Situ Micro-Compression[5] – 0.3 µm & 3.0 µm particles

- Single crystal, ultra pure 0.3µm & 3µm, α-Al_2O_3 particles.
- A Hysitron PI85 SEM Picoindenter[6] and the SEM at 5.0 kV were used. Compression done in a ***displacement control*** mode.
  - 0.3 µm particles → 3 µm Ø flat punch tip, **15 nm/s** displ rate.
  - 3.0 µm particles → 6 µm Ø flat punch tip, **8 nm/s** displ rate.
- A Hysitron PI95 TEM Picoindenter with a 1 µm diameter flat punch tip and the a JEOL 2100 LaB_6 TEM[7] at 200 kV were used. Compression done in ***open loop*** mode with the loading rate of 10 µN/s (approx. **< 2 nm/s** displ rate).

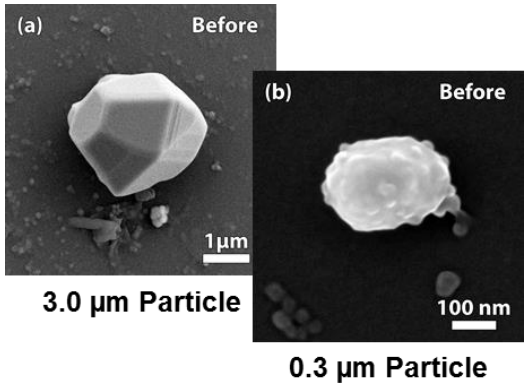

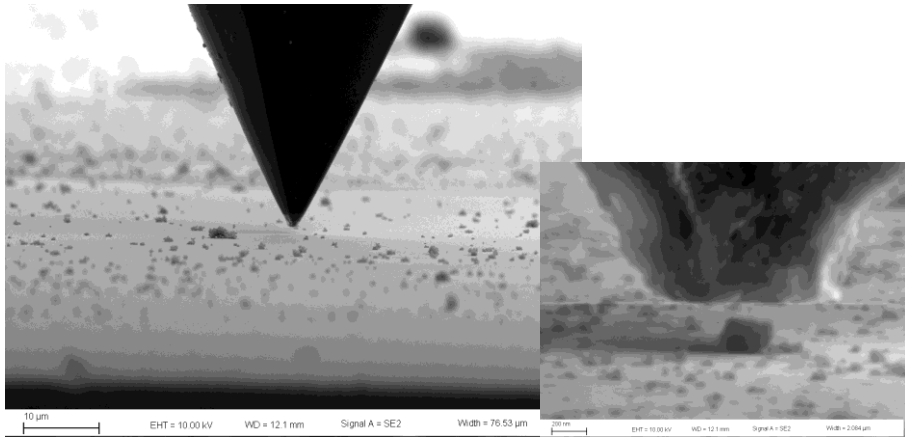

In situ SEM micro-compression on 0.3µm particle

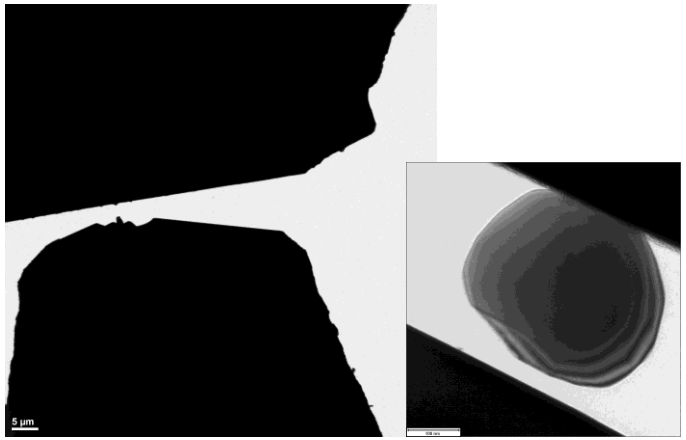

In situ TEM micro-compression on 0.3µm particle

[5] Sarobol, P., *et al*., *SAND2014-18127*, (2014).
[6] Hysitron I (2013) SEM Picoindenter User Manual. Revision 9.3.0913 edn.
[7] Hattar, K., et al., Nuclear Instruments and Methods in Physics Research B. Vol. 338, (2014), pp. 56–65.

In Situ SEM micro-compression – 3.0 µm

Sandia National Laboratories

Displacement control, Strain rate ~ 0.003 s^{-1}

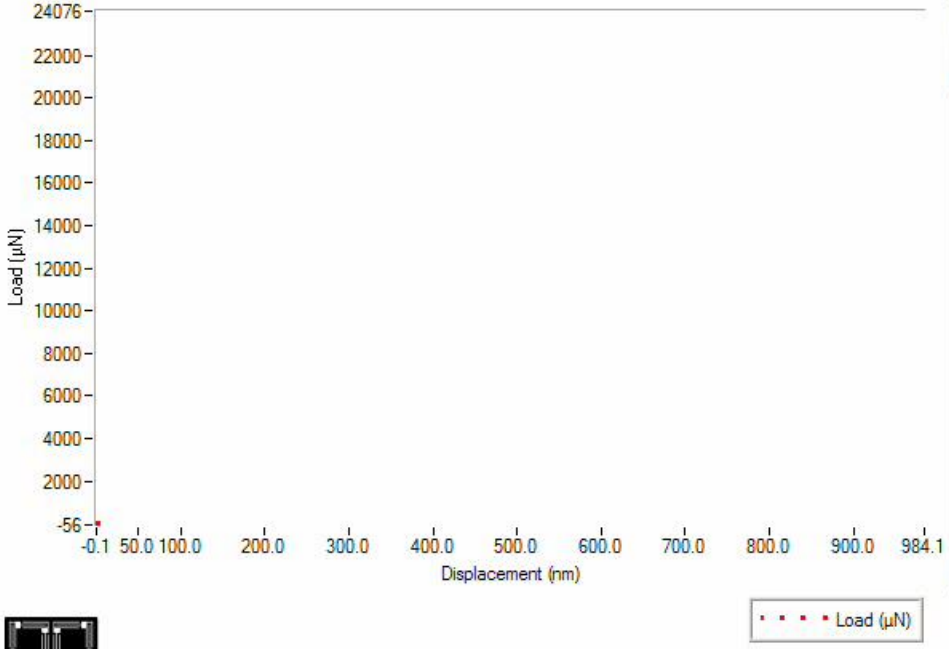

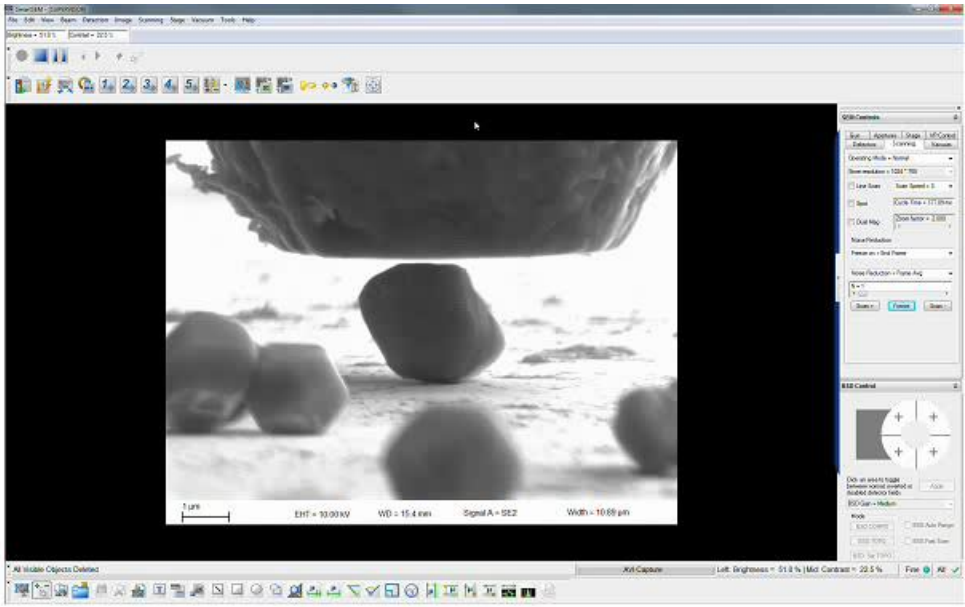

HYSITRON™

- Compressed 4 particles
- No observable shape change prior to fracture and fragmentation
- Displacement excursion corresponded to a fast fracture event
- Strain Energy Density before Fracture ~203 MJ/m^3
- Strain at fracture ~7%

Tip could not keep up with large displacement gained during fracture.

In Situ SEM micro-compression – 0.3 µm

Sandia National Laboratories

Displacement control, Strain rate ~ 0.05 s^{-1}

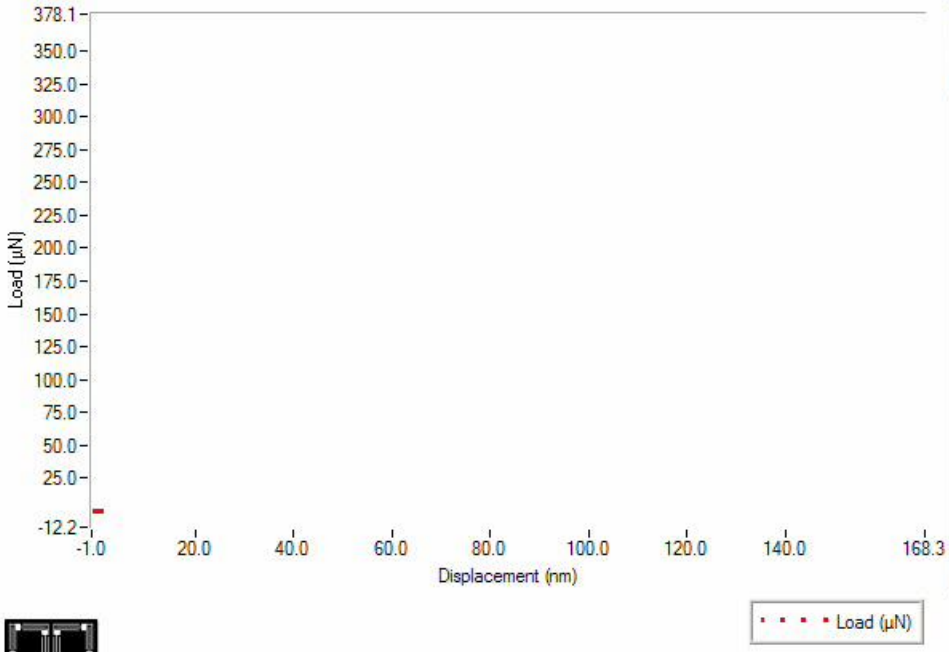

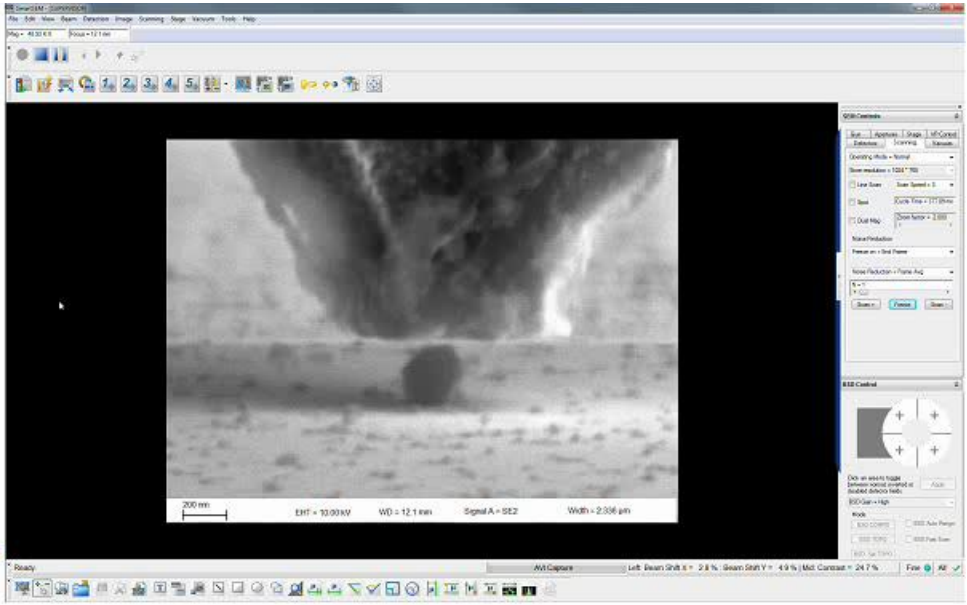

HYSITRON™

- Compressed 4 particles
- Significant plastic deformation/ shape change and stayed intact
- Displacement excursion corresponded to??? *Ex situ* observation
- Strain Energy Density before displacement excursion ~675 MJ/m^3
- Strain at displacement excursion ~16%

Tip could not keep up with large displacement gained during fracture.

Ex Situ SEM observation – 0.3 µm

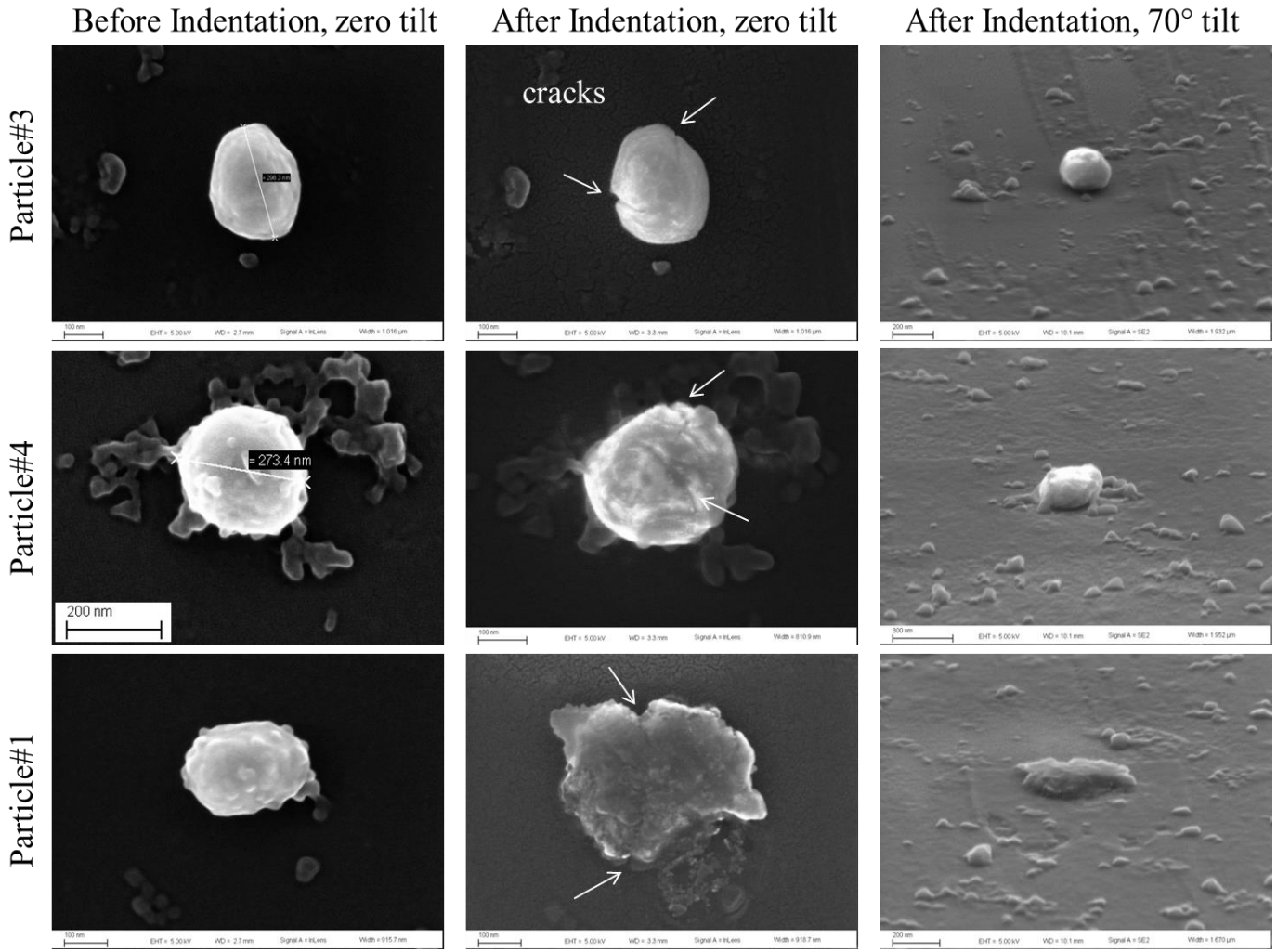

~307 µN
Max load

~420 µN
Max load

Extreme
Loading

Different deformation behavior and load at first fracture may differ from particle-to-particle due to orientation differences and different pre-existing defect densities. However, overall, the sub-micron sized alumina particles exhibited significant plastic deformation before fracture.

In Situ TEM Micro-Compression – 0.3µm

Sandia National Laboratories

Diameter ~ 0.38 µm, Open loop, Strain rate ~0.005 s^{-1}

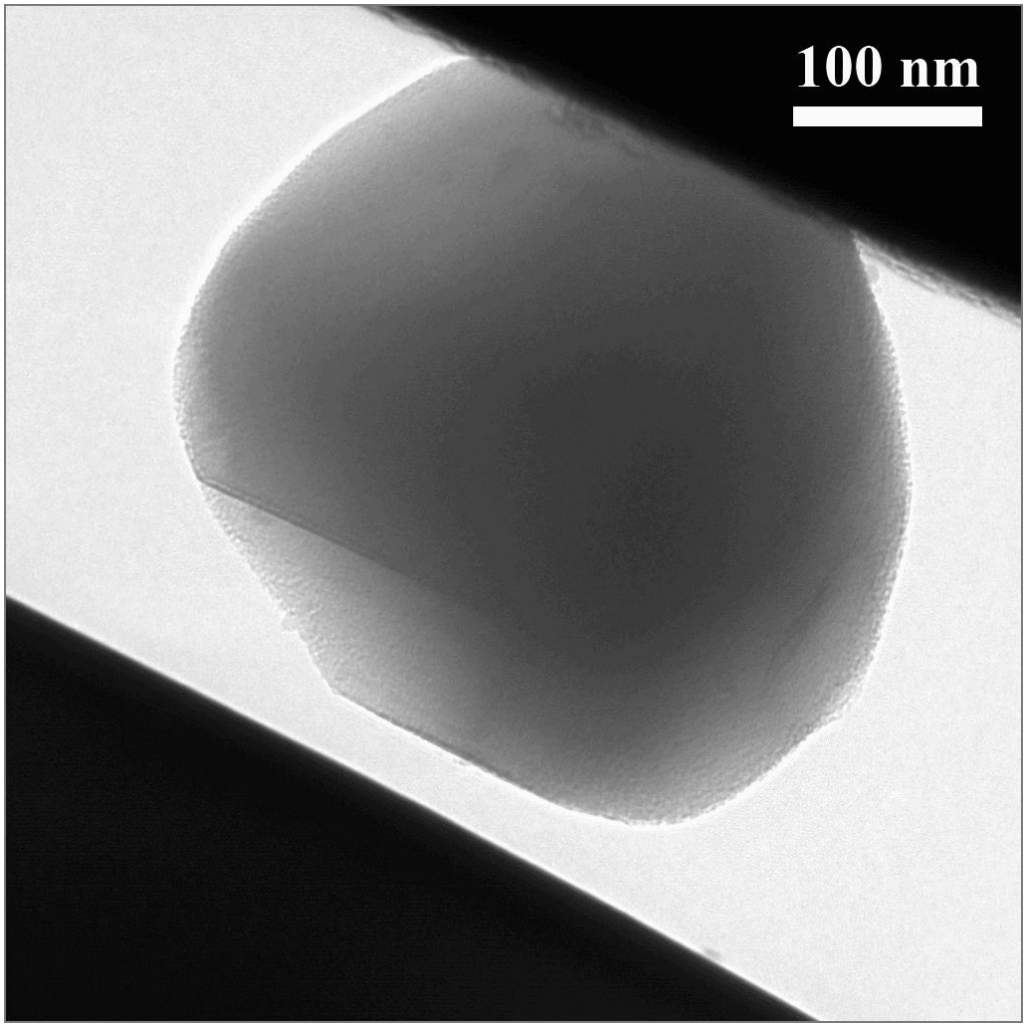

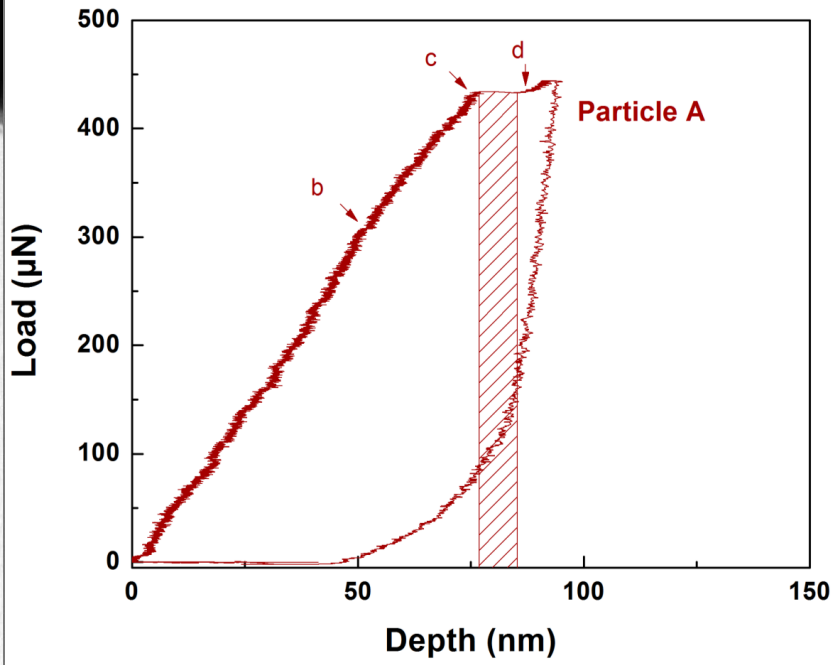

In Situ TEM Micro-Compression – 0.3µm

Sandia National Laboratories

Zone axis near $[\bar{2}\ 5\ \bar{3}\ 2]$

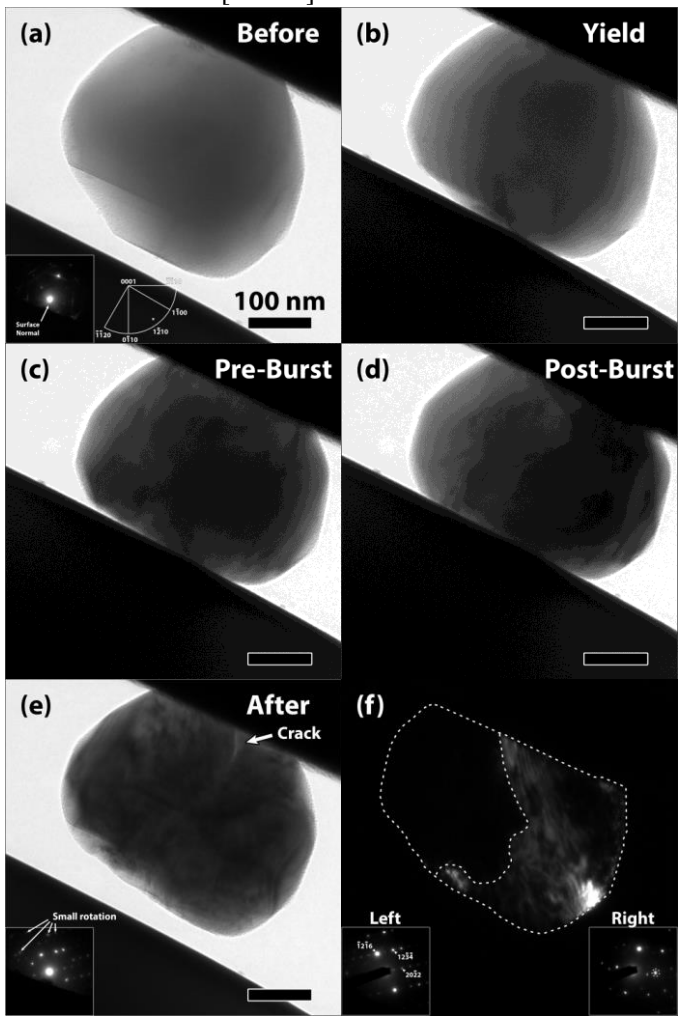

Two halves related by slight rotation, both near $[\bar{1}\ 2\ 1\ 6]$ zone axis

- Stored Energy Density Before Fracture = 573 MJ/m^3

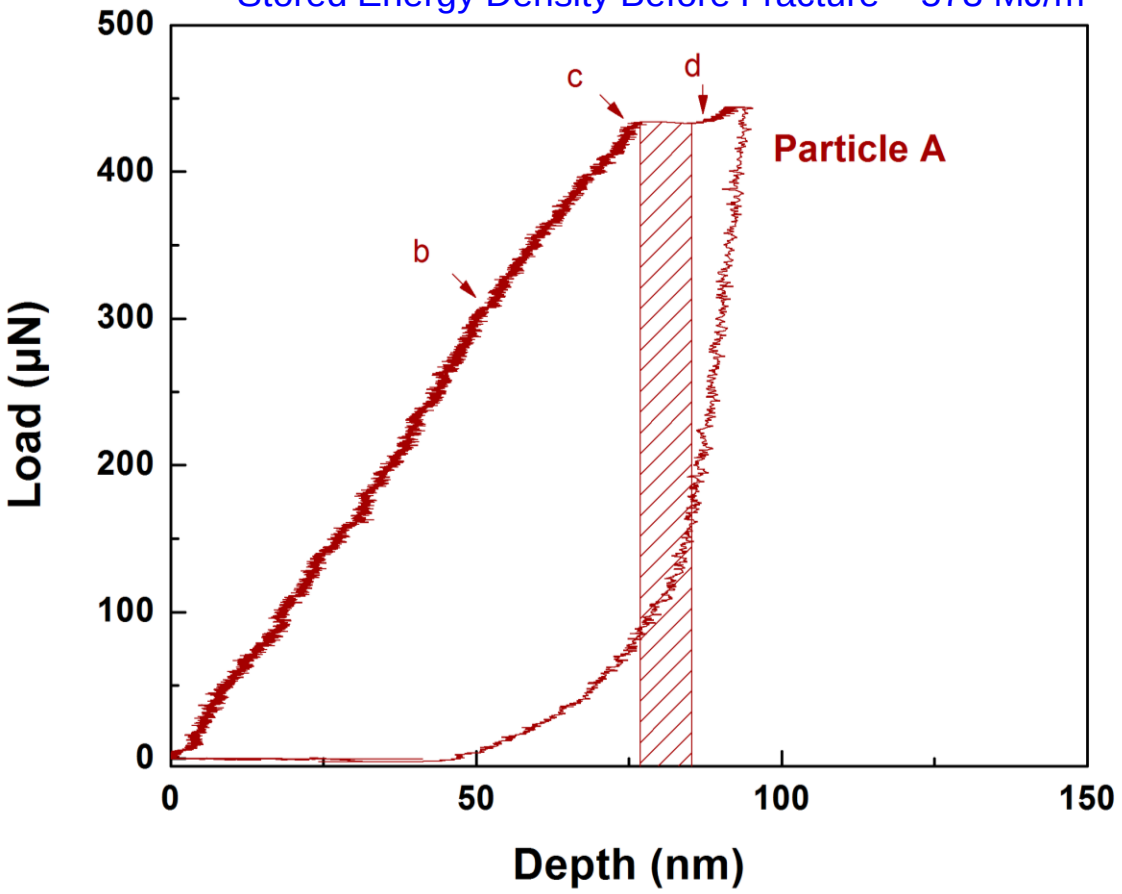

- Pre-burst plasticity: large regime with **high dislocation activity** (nucleation and moving through particle).
- **Crack nucleation and propagation** leading to through-particle fracture.

Predicted Particle Velocity

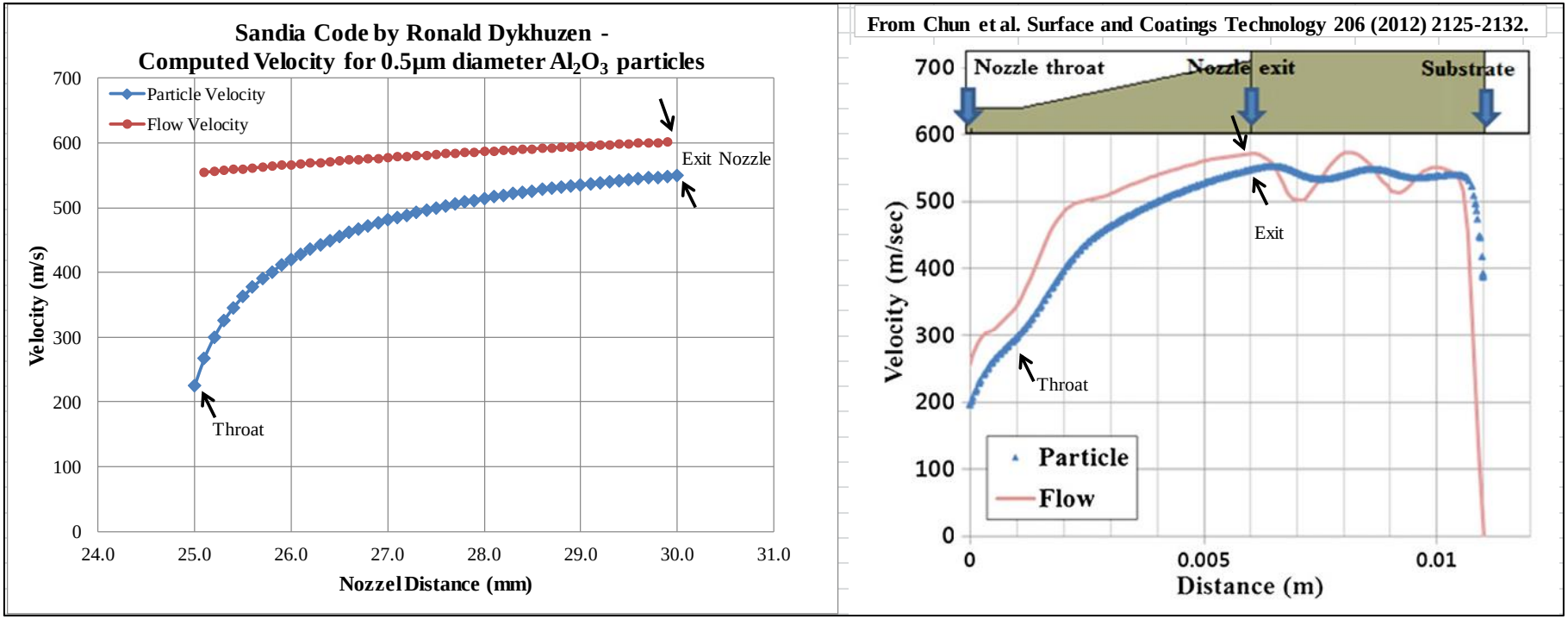

Calculated gas and particle velocity along the nozzle using parameters given by Chun et al (1).
Left, SNL's Dykhuizen et al.'s 1-D code (2-4) showing exit velocity of 562 m/s
Right, from Chun et al.'s CFD modeling (1) showing exit velocity of ~550 m/s.

1. Chun DM, Ahn SH. " Deposition mechanism of dry sprayed ceramic particles at room temperature using a nano-particle deposition system," Acta Materialia, 2011, 59, pp. 2693-703
2. Dykhuizen RC and Smith MF, "Gas Dynamic Principles of Cold Spray," JTST, 1997, 7, pp. 205-212.
3. Dykhuizen RC, Smith MF, Gilmore DL, Neiser RA, Jian X, and Sampath S, "Impact of High Velocity Cold Spray Particles," JTST, 1999, 8, pp. 559-564.
4. Gilmore D., Dykhuizen RC, Neiser RA, Roemer TJ, and Smith MF, "Particle Velocity and Deposition Efficiency in the Cold Spray Process," JTST, 1999, 8, pp. 576-582.